Endogenous Screening and Health Behaviors*

Michael Darden and Alex Hoagland

September 11, 2026

Abstract

Health screening is valuable not only for what it detects but for how the resulting information changes behavior. We study this complementarity between screening and prevention in the context of lung cancer screening and cigarette smoking, estimating a dynamic model of joint screening and smoking decisions from a randomized information experiment, electronic health records, and population data. In the model, a favorable screen reduces smoking through a value-of-life effect because, in this context, prevention is more valuable when cancer-free. A one-time screen at age 45 lowers smoking by 11.9% and lifetime lung cancer incidence by 2.2%. Exploiting this channel, expanding screening eligibility along the smoking-history margin, from 20 to 10 pack-years, generates large welfare gains despite the low cancer risk of the newly covered smokers. More generally, we derive sufficient statistics that determine whether screening and health behaviors are complements, and when that complementarity improves health and welfare.

Keywords: Health screening; preventive behavior; smoking; dynamic choice; information and belief updating; structural estimation

JEL Classification: I12, I18, D83, D91, C61

*Darden: Johns Hopkins University and NBER. Hoagland: University of Toronto. We are grateful to Justin Sydnor and Dan Zeltzer for helpful comments, as well as seminar participants at ASHEcon 2026 and the 2026 Midwestern Health Economics Conference for their useful feedback. Funding was provided by the Carey Business School at Johns Hopkins University. We have no conflicts of interest to report. Shadi Varmazyari provided superb research assistance.

1 Introduction

Health screening is both a diagnostic technology and an information technology. Its value depends not only on who is screened and what the test detects, but on how the resulting information reshapes subsequent health behavior. We develop and estimate a dynamic learning model in which individuals jointly choose whether to screen and whether to invest in other forms of prevention. In the model, screening affects health through two channels. The first is diagnostic: screening advances the timing of detection and treatment, consistent with recent work focused on selection into screening, where the benefit to marginal screeners can differ sharply from the average (Einav et al., 2020). The second channel is behavioral: by changing beliefs about future health, screening changes the return to prevention. The value of screening then depends not only on disease risk and test accuracy but on how responsive marginal screeners are to health information, and the sign of that response is a priori ambiguous. A favorable screening result lowers perceived risk, which may crowd out costly prevention through a moral-hazard effect; but it also raises expected survival, and thus the value of a longer life, strengthening the incentive to invest. Which force dominates is an empirical question, and its answer governs whether screening and prevention are substitutes or complements and the overall value of screening.

We study these mechanisms in lung cancer screening, a setting in which screening recommendations are explicitly tied to cigarette smoking, a behavior that individuals can also change. Lung cancer is the third most common cancer diagnosis in the United States and the leading cause of cancer death. Early detection is especially valuable, as five-year relative survival falls from 65.5% for localized disease to 10.5% for distant-stage disease. United States Preventive Services Task Force (USPSTF) guidelines recommend annual low-dose computed tomography (LDCT) screening based on age and smoking history, yet screening prevalence is only 24.5% in the recommended population (Burus et al., 2026).[1] At the same time, nearly half of all lung cancer screening occurs among people who do not meet USPSTF guidelines (Darden and Hoagland, 2025), which might suggest little room for policy to raise welfare by broadening eligibility.[2] We reach the opposite conclusion. The value a marginal screener derives from screening, through the reduction in smoking it induces, is large enough that expanding eligibility for cost-sharing-exempt screening substantially improves welfare.

To estimate the model, we combine novel experimental variation with rich clinical and population data. We conduct a randomized information experiment among 4,000 current and former smokers that identifies

[1] Current USPSTF guidelines recommend screening for adults ages 50 to 80 with at least a 20 pack-year smoking history who currently smoke or quit within the past 15 years.

[2] Typically, Medicare follows USPSTF guidelines and covers services and procedures that receive a B grade or higher. Following USPSTF's 2021 updated lung cancer screening guidelines, Medicare issued a National Coverage Determination covering LDCT lung cancer screening. Most private payers and state Medicaid offices also follow these guidelines. See the timeline in the Appendix for more information.

preferences, beliefs, and expectations. It randomly varies information about screening prices, stigma-related barriers, and test quality, identifying key components of screening demand. It also elicits how current smokers expect to change their smoking after a favorable screening result, which lets us separate a moral-hazard effect from a value-of-life response. Our model shows that this experimental response to information is a sufficient statistic to separately identify which of the two effects will dominate behavioral responses to information. Our evidence on intention to quit smoking is consistent with Brain et al. (2017), who present revealed preference, large-scale randomized controlled trial evidence on smoking behavior following both positive and negative lung cancer scans. We combine experimental survey moments with three large data sources. From Truveta's standardized electronic health records, spanning more than 100 United States health systems, we measure real-world diagnostic outcomes, including false positives. From the National Lung Screening Trial, we recover plausibly policy-invariant clinical transition probabilities. From the Behavioral Risk Factor Surveillance System (BRFSS), we identify smoking preferences and addiction patterns. We estimate the model by simulated GMM, matching these experimental and observational moments to model simulations.

Simulations of the estimated model show how the welfare and health consequences of screening depend critically on the behavioral response to information. For a population above age 40 with some smoking history, a one-time universal screen at age 45 reduces smoking by 11.9% relative to a counterfactual without screening. Those who smoke less because of screening spend 7.5 additional years smoke-free. Not all of this cessation is permanent, and we estimate that by age 65 only about one-third of those who quit at 45 remain abstinent. Even so, the resulting reductions in smoking cause a 2.2% decline in lung cancer incidence later in life, and these health gains carry through to longevity. Among those whose cancer incidence falls, 80.2% live longer, by an average of 7.9 years. These magnitudes are consistent with the smoking and longevity literature that finds survival curves to be roughly equivalent between never smokers and smokers who quit before age 50 (Darden et al., 2018; Doll et al., 2004). Importantly, these effects can be induced through existing policy levers, including modifying screening prices and expanding USPSTF eligibility along either the age or smoking-history margin. Taken together, the results imply that screening information complements prevention rather than crowding it out, and that screening recommendations should account for both selection into screening and the endogenous smoking response to favorable health information.

We calculate the increases in *ex ante* lifetime expected utility that expanding screening coverage might generate, and we decompose them into welfare gains from changes in preventive behavior (such as quitting) and gains from other screening benefits (such as improved cancer detection). We consider two coverage expansions. The first exempts cost-sharing for qualifying individuals at age 45 rather than 50, and the second lowers the smoking-history threshold from 20 pack-years to 10. These expansions generate large welfare gains. Across the model population, unconditional welfare rises by 0.4 to 0.6% of lifetime discounted utility at age 40, equivalent to between $60,000 and $70,000 per person over the lifetime. Because roughly one fourth of

Americans have a smoking history by age 40, this implies a total gain of roughly $73 to $83 billion for an average 40-year-old cohort. About one fifth of this gain is attributable to changes in smoking behavior rather than to improved detection alone.

Taking inspiration from both Grossman (1972) and Ehrlich and Becker (1972), a large economic literature has studied preventive healthcare as an investment in promoting better health.[3] Our work contributes to this literature by emphasizing the joint determination of preventive care and other health behaviors in an intertemporal setting. In our framework, preventive care not only affects health directly but also changes beliefs, and therefore the returns to other health investments, particularly those characterized by addiction (Becker and Murphy, 1988; Gruber and Kőszegi, 2001; Bernheim and Rangel, 2004; Gul and Pesendorfer, 2007; DeCicca et al., 2022). While we study this interaction in the context of lung cancer screening and smoking, the underlying mechanism applies more broadly to settings in which individuals jointly choose screening, lifestyle changes, and preventive treatments. The clearest example is the literature on HIV/AIDS and risky behavior, where the sign of the behavioral response to information is contested. Thornton (2008) uses randomized incentives to learn HIV status and finds no significant condom-use response to learning one is HIV-negative, while Gong (2015) finds that individuals surprised to learn they are HIV-negative reduce risky sexual behavior, consistent with a value-of-life effect. Using a structural learning framework similar to ours, de Paula et al. (2014) find the opposite direction, with downward revisions in the probability of being HIV-positive raising risky behavior, while Delavande and Kohler (2016) find that expectations about mortality, rather than about living with HIV, drive risky sexual behavior. Finally, Oster (2012) finds a larger behavioral response to HIV risk among those with lower competing mortality; our model incorporates competing risk directly by jointly modeling lung cancer, other chronic conditions, and mortality.

This paper contributes to the economics of information by modeling health screening as a dynamic information technology that shapes what agents learn, when they learn it, and how they update beliefs prior to making health investments. In doing so, we connect to a large structural literature on learning and information acquisition. A first strand studies how agents update beliefs about product quality or health risk over time and how these beliefs shape behavior (Crawford and Shum, 2005; Hoagland, 2026). A second strand embeds learning in dynamic choice environments, emphasizing how forward-looking behavior interacts with information accumulation (Chan and Hamilton, 2006; Ching et al., 2013; Darden, 2017; Anderson et al., 2024). Relative to this work, we focus on screening as an endogenous information choice, in which agents decide not only how to act given beliefs but also when and whether to acquire new information. In our model, this generates an equilibrium screening threshold, with individuals optimally selecting the timing and frequency of information acquisition as part of their broader health investment problem.

Finally, we make a methodological contribution to the estimation of structural models with complex,

[3] Among many examples, see Gilleskie (1998); Miguel and Kremer (2004); Chandra et al. (2010); Baicker et al. (2015); Alsan et al. (2019); Newhouse (2021).

irregular objective functions. We introduce a machine-learning–assisted warm-start procedure for simulated GMM that uses flexible prediction algorithms to identify economically meaningful and computationally efficient starting values. The approach combines a large-scale, design-based exploration of the parameter space with supervised learning to approximate the mapping from parameters to model moments and to screen out regions associated with corner or degenerate solutions. In contrast to recent work that uses machine learning to approximate or replace the structural estimator itself (Catherine and Ebrahimian, 2024; Duarte and Fonseca, 2023), we preserve the standard GMM framework and use machine learning only to guide initialization. Our approach is also complementary to recent efforts to use machine learning to select or weight moments in structural estimation (Zila and Kukacka, 2023). This strategy improves convergence and stability in settings where solving the model is costly and the objective surface is highly non-convex, and is broadly applicable to a wide class of dynamic structural models, including life-cycle models like our own (Capatina and Keane, 2026).

2 Conceptual Model

We develop a simple model that rationalizes joint screening and health prevention behavior. In this framework, we isolate a mechanism for screening that lies in revealed information enabling the agent to change the optimal level of prevention. The model is intentionally kept general, abstracting from important mechanisms such as preferences over screening (i.e., stigma); these mechanisms are incorporated below.

Because prevention and screening are chosen simultaneously, we focus on two periods of a life-cycle framework to highlight how changing beliefs in one period cause changes in prevention in the next period. The result of the model is a Jensen gap that describes the expected value of screening relative to its price. Importantly, the model assumes rational expectations and time consistency, meaning that the value of screening is generated entirely by the resolution of uncertainty.

Consider an agent with health type $\omega \in \{G, B\}$, which we assume is time-invariant and unobserved to the agent. There are two periods, $t = 1, 2$, discounted at $\beta \in (0, 1]$. At the beginning of period $t = 1$, the agent holds beliefs of "bad" health:

$$b \equiv \Pr(\omega = B)$$

Given b, the agent simultaneously selects whether to undergo screening, x_1, and how much prevention, a_1 to consume:

$$\underbrace{x \in \{0, 1\}}_{\text{screen}} \qquad \text{and} \qquad \underbrace{a \geq 0}_{\text{prevention}} .$$

Screening may be purchased at price p, and the cost of prevention is a continuous and convex function of the

level of prevention, $c(a_t)$, where $c' > 0$ and $c'' > 0$.[4]

If $x_t = 0$, no signal arrives, and beliefs remain at b. When $x_t = 1$, a screen returns a binary signal $z_t \in \{g, b\}$ (negative or positive) with probabilities:

$$\Pr(z_t = b \mid \omega = B) = q_B, \qquad \Pr(z_t = g \mid \omega = G) = q_G,$$

These probabilities reflect the imperfection of the screening technology, which is to say that the agent is aware of the likelihood of false positives and false negatives. Given signal z_t, agents update beliefs to a posterior belief ($\mu_z \equiv \Pr(\omega = B \mid z)$) based on Bayes' rule:

$$b_g \;=\; \frac{(1-q_B)\,b}{(1-q_B)b + q_G(1-b)} \;<\; b \;<\; b_b \;=\; \frac{q_B\,b}{q_B\,b + (1-q_G)(1-b)}.$$

We assume that beliefs are a martingale such that $\sum_z Pr(z|b)b_z = b$. Simultaneity is within a period: the screening result is not yet known when x and the current period's prevention are chosen, so contemporaneous prevention cannot respond to it. The signal from screening instead reshapes next period's belief, and hence next period's prevention.

Prevention is valuable for survival from one period to the next, the probability of which we assume is linear in prevention:

$$S(\omega, a_t) = (s_\omega + \delta_\omega\, a_t) \in (0,1), \qquad s_G > s_B \geq 0, \qquad \delta_G, \delta_B \geq 0. \tag{1}$$

The same technology governs both transitions: survival from period 1 to period 2 (as a function of a_1) and survival past period 2 (as a function of a_2). Define $\bar{s}(b) = (1-b)s_G + b\,s_B$, $\bar{\delta}(b) = (1-b)\delta_G + b\,\delta_B$, and $\bar{S}(b,a) = \bar{s}(b) + \bar{\delta}(b)a_t$, which characterize how beliefs over health state ω feed through to beliefs about survival.

In any given period, being alive yields a state-dependent flow utility $\bar{u}(b) = (1-b)u_G + b\,u_B$. Furthermore, surviving beyond period $t = 2$ entails a cash-out value of Ω.

Prevention under uncertainty. In period $t = 2$, because the cash out term Ω is invariant to the state, screening represents a pure cost. We therefore assume without loss of generality that $x_2^* = 0$. When prevention is chosen in period $t = 2$, the state ω is unknown, so a_2 solves an expected-utility problem under the prevailing

[4]Cost convexity is a key assumption in this framework, so that the marginal costs of prevention increase at an increasing rate. This is a natural assumption for preventive health behaviors, where the marginal costs of small amounts of prevention (e.g., minimal exercise) may be dwarfed by the marginal costs of more significant investments. Under a rational addiction framework (e.g., quitting smoking), these differences may be further compounded.

belief b:

$$V_2(b) = \max_{a \geq 0} \left\{ \bar{u}(b) - c(a) + \beta \, \bar{S}(b, a) \, \Omega \right\}. \tag{2}$$

The prevention first-order condition is a value-of-life condition,

$$c'(a) = \beta \, \bar{\delta}(b) \, \Omega \qquad \Longrightarrow \qquad a^\star(b) = (c')^{-1}\Big(\beta \, \bar{\delta}(b) \, \Omega\Big), \tag{3}$$

so prevention rises with the marginal survival return $\bar{\delta}(b)$ and with the payout Ω it secures. Writing the prevention surplus $G(\delta) \equiv \max_a\{\beta\delta\Omega a - c(a)\}$:

$$V_2(b) = \underbrace{\bar{u}(b) + \beta \, \bar{s}(b) \, \Omega}_{\text{affine in } b} + G\Big(\bar{\delta}(b)\Big). \tag{4}$$

The shape of the prevention surplus $G(\bar{\delta})$ foreshadows much of the results below. Recall that $\bar{\delta}$ is the belief-weighted assessment of the return to prevention. As $\bar{\delta}$ increases, health state beliefs must be adjusting towards the state with the higher return. At the optimal level of prevention, $G' = a_2^*(\bar{\delta})\beta\Omega > 0$, which implies that utility from prevention increases as beliefs adjust towards the state with the higher return. Furthermore, note that the convexity of G is determined by the condition $G'' = \frac{da^*}{d\bar{\delta}} \cdot \beta\Omega = (\beta\Omega)^2/c''$, which is positive because c'' is positive. That is, if we have cost convexity for c, then G is also convex. This has direct implications on the value of screening.

Optimal Screening. In period $t = 1$, the continuation value V_2 depends on beliefs. Screening x_1 is chosen simultaneously with a_1; it cannot steer a_1 through z, but it does raise the informativeness of the period-2 belief. Comparing the two screening choices,

$$J^0(b) = \max_{a_1 \geq 0} \Big\{ \bar{u}(b) - c(a_1) + \beta \, \bar{S}(b, a_1) \, V_2(b) \Big\}, \tag{5}$$

$$J^1(b) = \max_{a_1 \geq 0} \Big\{ \bar{u}(b) - c(a_1) + \beta \, \bar{S}(b, a_1) \, E_z V_2(b_z) \Big\}, \tag{6}$$

where $E_z V_2(b_z) = \sum_z P(z|b) V_2(b_z)$.

The result is that a person screens in $t = 1$ if and only if $J^1(b) - J^0(b) > p$. There are two clear complementarities between screening and prevention. First, define the Jensen gap that results from differencing the expected continuation values

$$\Lambda(b) \;\equiv\; E_z V_2(b_z) - V_2(b) \;=\; E_z \, G(\bar{\delta}(b_z)) - G(\bar{\delta}(b)). \tag{7}$$

This is positive if G is convex as discussed above. Second, if $\Lambda(b) > 0$, there is an incentive to increase period

1 prevention to balance the period 1 first-order condition. That is, if one expects a value from screening, the return to current prevention increases.

Testable Implications. The Jensen gap in Equation 7 is governed by three sufficient statistics, which collectively determine its sign (and hence, the impact of screening on future prevention):

1. $\underbrace{\rho \equiv \frac{da^\star}{d\delta} = \frac{\beta\Omega}{c''}}_{\text{prevention responsiveness}}$
2. $\underbrace{I \equiv b_b - b_g}_{\text{screen informativeness}}$
3. $\underbrace{D \equiv \delta_B - \delta_G}_{\text{state-dispersion of returns}}$.

First, consider the effect of changes in beliefs on optimal preventive behavior, denoted by ρ. This depends on the shape of the cost function for preventive behavior. If prevention does not respond to updated beliefs, then G is linear, $\rho = 0$, and screening is a pure cost. If, on the other hand, $\rho > 0$, then beliefs directly impact the future value of prevention. Second, consider the informativeness of the screening technology. If an agent correctly or incorrectly believes that the rate of false positives is sufficiently high, then a positive signal may not move beliefs, which leaves b unchanged and, as a result, $\bar{\delta}$ unchanged. The final sufficient statistic, $(\delta_B - \delta_G)$, captures the relative marginal value of prevention in the survival equation across health states. That is, the state dispersion of return to prevention implicitly weighs the tradeoff between the value inherent in continuation of life against any potential moral hazard effects.

To build intuition on these statistics, consider a person who elects to screen, and who receives a negative screening. If the signal is informative, this causes the belief in the bad health state to update downward to $b_g < b$. Beliefs are important in the model because they affect how the agent forecasts survival. Because $d\bar{\delta}/db = \delta_B - \delta_G$, a fall in b causes $\bar{\delta}$ to fall by $\delta_B - \delta_G$, which causes G to change by $a_2^*\beta\Omega$. Thus, the sign of a negative screen on preventive behavior depends on the sign of $\delta_B - \delta_G$. If $(\delta_B - \delta_G) < 0$, then a negative screen reduces b, which increases G. We call this the value-of-life effect, and, in this case, if G is convex, then the negative screen results in more prevention. In contrast, $(\delta_B - \delta_G) > 0$, then a negative screen leads to less prevention through a moral hazard effect. Finally, note that $V_1(b)$ is a money-metric lifetime value, so $J^1(b) - J^0(b)$ is the willingness to pay for a screen and $J^1(b) - J^0(b) - p$ its net private value. Aggregated over agents, this term represents the numerator of the marginal value of public funds of a change in screening policy.

Our framework describes screening as an information technology that allows individuals to update their behavior, clearly connecting screening and prevention. Ultimately, the sufficient statistics above are empirical questions that depend on context.

3 Lung Cancer Screening and Smoking

We apply our framework to lung cancer screening and cigarette smoking, a context in which the marginal return to prevention is almost certainly higher when free of cancer (i.e., $(\delta_B - \delta_G) < 0$). Conditional on lung cancer, the 5-year survival rate is 28.6%, falling to 10.5% for diagnoses with more distant cancer.[5] These statistics are suggestive of a small return to prevention in a state of cancer (i.e., δ_B is small). However, survival curves are roughly equivalent between never smokers and smokers who quit before age 50, and expected loss of longevity from continuing smoking ranges from a model-implied estimate of 4.3 years to an unconditional estimate of 10 years (Darden et al., 2018; Doll et al., 2004); this suggests a relatively large return to prevention (i.e., smoking cessation) when free of cancer. It also suggests that a crucial period for cessation — in midlife, prior to age 50 — coincides with a set of disputed ages for lung cancer screening, as we discuss below. The model implication of a large δ_G and small δ_B is a strong "value-of-life" effect, in which a negative screen encourages smoking cessation. Thus, we focus our empirical work on understanding how those on the margin of screening react to information with respect to their smoking behavior. In this section, we review where the relevant margins lie with respect to lung cancer screening policy.

In 1996, the United States Preventive Services Task Force gave LDCT lung cancer screening a "D" grade (U.S. Preventive Services Task Force, 2004). The report cited evidence that screening may detect lung cancer at an earlier stage, but it cited poor evidence on its effectiveness regarding lung cancer survival, and it highlighted a lack of randomized-controlled trial evidence. Following this determination, in 2002, the National Lung Screening Trial (NLST) began, enrolling over 53,000 participants between the ages of 55 and 74 who had at least 30 pack-years of smoking history.[6] Participants at one of ten locations were randomized into LDCT screening or chest radiography, and they received three screenings over roughly three years. The participants were followed through 2010. In the LDCT arm, there were more lung cancer diagnoses in the LDCT group (645 vs. 572), but there were fewer lung cancer deaths (247 vs. 309) (The National Lung Screening Trial Research Team, 2011).

The NLST had a transformative effect on lung cancer screening policy in the United States. In 2013, USPSTF revised their recommendation for LDCT to a "B" grade for adults 55 to 80 with 30+ pack-years and who currently or recently (within 15 years) have smoked (U.S. Preventive Services Task Force, 2014). The recommendation concluded that screening should be stopped after a person has been a non-smoker for 15 years. Following the USPSTF update, Centers for Medicare and Medicaid Services (CMS) issued a National Coverage Determination for LDCT screening, ensuring Medicare coverage for LDCT lung cancer screening for the first time. The criteria for coverage included the age and smoking history requirements from the USPSTF recommendation, in addition to screening counseling and a shared decision-making visit to be

[5] https://www.cdc.gov/united-states-cancer-statistics/publications/lung-cancer-stat-bite.html

[6] One pack-year of smoking history is equal to smoking one, 20-cigarette pack of cigarettes per day for an entire year.

furnished by a physician. Furthermore, the beneficiary needed to be free of cancer or other health condition that "substantially limits life expectancy or the ability or willingness to have curative lung surgery." (Centers for Medicare & Medicaid Services, 2015)

The shared decision-making requirement was controversial, mainly because shared decision-making was not required for coverage of other cancers (Volk et al., 2020). Furthermore, comments to CMS indicated that this additional step required for a covered lung screening represented a barrier to access, and it was deemed to be an overly complex requirement (Volk et al., 2026). In defending this requirement, CMS cited important heterogeneity in costs and benefits across individuals. In particular, the associated National Coverage Analysis (Centers for Medicare & Medicaid Services, 2015) stated that,"Shared decision-making is important for the population for whom screening is recommended. The benefit of screening varies with risk because persons who are at higher risk because of smoking history or other risk factors are more likely to benefit."

Following evidence of lower false positives and of greater survival benefits relative to the NLST, USPSTF expanded recommended LDCT screening to those between the ages of 50 and 80 with a 20-pack year smoking history (U.S. Preventive Services Task Force, 2021). CMS' National Coverage Determination quickly followed in 2022, broadening coverage of LDCT screening to the expanded population while preserving the shared-decision making requirement (Centers for Medicare & Medicaid Services, 2022). Both traditional Medicare and Medicare Advantage enrollees who meet the expanded criteria may receive LDCT screening with no cost-sharing. Furthermore, individuals who meet the expanded criteria and who qualify for Medicaid may receive screening with no cost-sharing. The Affordable Care Act requires non-grandfathered private plans to cover "A" or "B" graded preventive services (Internal Revenue Service et al., 2010), ensuring coverage in most large individual and group insurance plans. For those outside of the current USPSTF recommendations, there is less evidence of insurance coverage. The typical LDCT screening costs between \$100 and \$400.[7] A timeline of these policy changes in lung cancer screening is provided in Appendix Section 1.

In the most recent 2021 USPSTF guidelines, screening is recommended to occur annually among those who meet the criteria, and screening is to be discontinued only after 15 years of smoking cessation. Of those recommended for screening according to the 2021 USPSTF guidelines, Bandi et al. (2024) find that only 18% have screened in the previous year. Similarly, Henderson et al. (2024) find that compliance with the USPSTF guidelines is only 16.4% of the recommended population. More recent evidence suggests that prevalence has increased to 24.5% (Burus et al., 2026). Darden and Hoagland (2025) find that nearly half (45.2%) of 2022 past-year screenings came from people outside of USPSTF guidelines.

[7]Estimate from the American Lung Association.

4 Structural Model of Lung Cancer Screening and Cigarette Smoking

We next turn to an application of the conceptual model, where we construct a dynamic model that rationalizes the observed incidence of lung cancer screening and cigarette smoking while allowing us to study how the marginal screening individual updates their preventive behaviors. We model screening and smoking decisions jointly in an environment with uncertainty about disease state and the quality of screening. We consider two forms of health: lung cancer and other chronic health. Unless lung cancer is advanced such that symptoms are obvious, the lung cancer state is unobserved by both the individual and the econometrician. Early stage lung cancer, if diagnosed, can potentially be cured, but advanced lung cancer cannot. Other health is a binary variable for the presence of any other chronic health condition, which captures the notion of competing risk.

Model Timing. Agents enter the model at age 40 and make annual decisions about health behaviors (smoking) and preventive care investments (lung cancer screening). All agents start with no cancer at age 40; this allows us to focus on endogenous selection into screening and preventive health behavior in the presence of imperfect information and competing health risks. We consider a time horizon through age 100, at which point death occurs with probability 1. Figure 1 presents the key stages of a representative age t, around which we structure our model presentation.

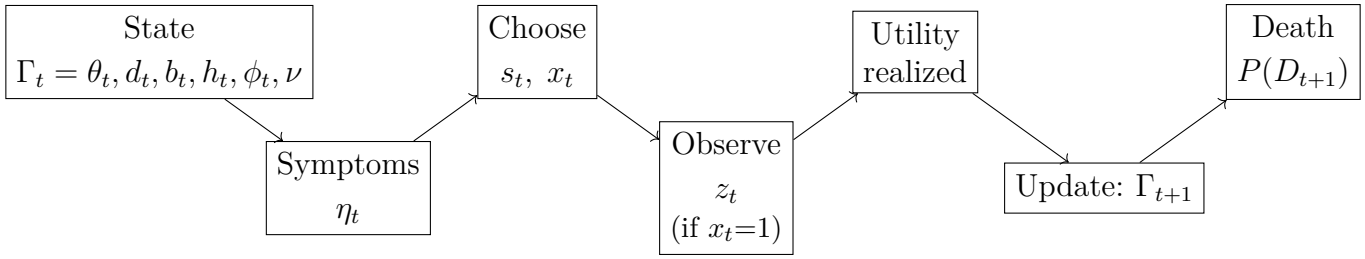


Figure 1: Model summary: timing of state, choices, information, and updating.

State Variables. Entering period t, an agent is characterized by a vector of state variables, Γ_t:

$$\Gamma_t = (\theta_t, d_t, b_t, h_t, \phi_t, \nu).$$

First, the lung cancer state corresponds to none, early-stage, and late-stage lung cancer, $\theta_t \in \{1, 2, 3\}$. Lung cancer is observed only when detected via screening. Hence, individuals also have a diagnosed state $d_t \in \{0, 1\}$, where it is possible for an agent to have cancer $\theta_t > 1$ without being diagnosed ($d_t = 0$). In

the absence of a diagnosis, agents have a subjective probability of any lung cancer, b_t.[8] Agents also are characterized by their smoking history, h_t; their other health state, $\phi_t \in \{1, 2\}$;[9] and a time-invariant type variable $\nu_i \in \{1, 2, 3, 4\}$ that characterize preferences for screening and beliefs about screening quality.

Next, an individual receives a draw of symptoms influencing both their beliefs about their lung cancer risk and their utility. Let η_t represent this draw, where:

$$\eta_t \sim F(\eta \,|\theta_t,\, \phi_t).$$

For tractability, we assume that symptoms are normally distributed, with mean and variance determined by the true underlying stage of cancer (including no cancer) and the presence of other health conditions. Based on this draw of symptoms, an individual's period-specific beliefs about any cancer are given by a conjugate posterior, where conditional beliefs about early- and late-stage cancer are approximately equally distributed as is true empirically. We calibrate these symptom draws to match prior literature, and allow for individuals to have endogenous, potentially idiosyncratic, beliefs about these two probabilities.[10]

Agent Choices. Conditional on state Γ_t and symptoms η_t, an individual simultaneously chooses whether to smoke cigarettes, s_t, and whether to screen for lung cancer, x_t. The action space is therefore given by

$$A_t = (s_t,\, x_t).$$

If a diagnoses has been already confirmed, we assume that screening is no longer a choice. In this case, we assume screening is automatic if cancer is early-stage to manage stage progression; if cancer is late-stage and diagnosed, then screening does not take place. If diagnosis has not occurred, at the time an agent makes smoking and screening decisions, there are two outcomes that are uncertain, both of which are observed if the agent chooses to screen. First, conditional on screening, they receive a signal of lung cancer $z \in \{0, 1\}$,

[8] If $d_t = 1$, then $b_t = 1$. We abstract from separate belief distributions of early- and late-stage lung cancer by using the fact that roughly 50% of new lung cancer diagnoses in the U.S. are late-stage.

[9] If $\phi_t = 2$, this indicates that an individual has chronic conditions that are highly co-morbid with lung cancer, including COPD and cardiovascular conditions. The risk of chronic condition onsets was determined using pooled health risk tables across these conditions (e.g., (National Cancer Institute, 2026)).

[10] In practice, we calibrate these symptom draws to match prior literature, such that the probability of observing symptoms is 0.033 if $\theta = 1$, 0.064 if $\theta = 2$, and 0.246 if $\theta = 3$. Given a binary draw for symptoms, rational belief updating of beliefs using Bayes' rule can be expressed as:

$$\tilde{b}_t|\eta = 1 : \frac{0.156\, b_t}{(0.156\, b_t + 0.033\, (1 - b_t)}$$
$$\tilde{b}_t|\eta = 0 : \frac{(1 - 0.156)\, b_t}{((1 - 0.156)\, b_t + (1 - 0.033)\, (1 - b_t)},$$

where the probability of symptoms given (any) cancer is 0.156 and the probability of symptoms given no cancer is 0.033.

the quality of which depends on its rates of false positives and false negatives. Define:

$$\Pr(z_t = 1 \mid \theta_t) = \begin{cases} \rho & \text{if } \theta_t > 1 \\ \lambda & \text{if } \theta_t = 1. \end{cases}$$

In this case, ρ is the accuracy of the test (i.e., sensitivity), the probability that the test reveals a true lung cancer. Thus, $1-\rho$ is the probability of a false negative. Similarly, λ is the probability of a positive test result in the absence of lung cancer (i.e., the rate of false positive), and $1-\lambda$ is the probability of a correctly negative test result. Both ρ and λ have objective average values that we estimate from Truveta data. However, what matters for behavior are an individual's subjective beliefs, $\hat{\rho}$ and $\hat{\lambda}$. We obtain these from our survey results.

Diagnosis, and subsequent treatment, collectively represent the second outcome. In the event of a positive signal, we assume that the agent undergoes additional testing. The subsequent testing, which incurs the same cost as the initial testing, is able to precisely determine the value of $\theta \in \{1, 2, 3\}$. If $\theta_t \in \{2, 3\}$, we assume that the agent is diagnosed ($d_t = 1$) and undergoes immediate treatment y at price p_y. Treatment affects the probability that early-stage θ will transition to late-stage cancer at the end of the period.[11] If the screening signal is positive (i.e., if $z_t = 1$) and the agent is free of lung cancer (i.e., $\theta_t = 1$), then we assume that subsequent testing, which is still costly, rules out lung cancer; in this case, $d_t = 0$.

Agent Payoffs. Utility is a function of the current state, the actions selected, and the outcomes of screening if chosen. Specifically, we specify a CRRA function of income net of expenditures on screening, smoking, and cancer treatment, and additively separable terms for smoking, screening, and treatment. Utility from smoking depends on its price p_s and the history of smoking h_t, which captures reinforcement (Becker and Murphy, 1988). The financial cost of screening is given by p_x, and the disutility of screening (including stigma) is given by γ_4. Taken together, utility is given by:

$$\begin{aligned} u(s_t, x_t; \Gamma_t) = & U_\theta + \frac{(W_t - p_s s_t - p_x x_t - p_y y_t)^{1-\gamma_0}}{1-\gamma_0} \\ & + (\gamma_1 + \gamma_2 h_t + \gamma_3 h_t^2) \cdot s_t \\ & - \sum_{v \in \nu} \gamma_{4,\nu}\, x_t\, \mathbb{1}\{\nu_i = v\} - \gamma_5 \tilde{p}_t - \gamma_6 \mathbb{1}\{\eta_t > 0\}. \end{aligned} \tag{8}$$

Utility is health state specific in the sense that we normalize the utility of death to 0. To ensure positive utility when alive, we also specify an additive parameter U_θ which varies by the presence of late-stage cancer ($\theta = 3$ vs. $\theta < 3$). These terms cardinalize the value of survival in each health state, and govern the continuation

[11] While we assume treatment occurs when there is late-stage lung cancer, this only affects utility generated while $\theta_t = 3$ and does not affect transition probabilities, as $\theta_t = 3$ is an absorbing state.

value of survival gains in each state. These terms, combined with the state dispersion in prevention returns, $\delta_B - \delta_G$, collectively determine whether the value-of-life channel dominates moral hazard, which depends on the relative magnitudes of $\delta_G U_{\theta<3}$ versus $\delta_B U_{\theta=3}$. We return to this in Section 6. These parameters are identified by an individual's willingness to engage in preventive care.

The second term represents CRRA utility over residual consumption, where wealth W_t is net of expenditures on smoking, screening, and treatment based on their respective prices and γ_0 is the typical CRRA risk aversion coefficient. Smoking affects utility directly through γ_1 and via linear and quadratic reinforcement effects with smoking history through γ_2 and γ_3, respectively. The summation term introduces type-specific heterogeneity in the marginal disutility of screening, with $\gamma_{4,\nu}$ indexing differential costs by individual type.[12] $\gamma_5 \tilde{p}_t$ captures utility loss from realized OOP medical spending, where $\tilde{p}_t$ is the expected price of both the initial test and any confirmatory testing.[13] Finally, γ_6 captures disutility from symptoms in each period.

State Transitions, Belief Updating, and Mortality. The state transition rules follow from behavior and screening outcomes. For lung cancer transitions, we make two simplifying assumptions. First, we assume the probability of late stage lung cancer conditional on no lung cancer is zero ($Pr(\theta_{t+1} = 3|\theta_t = 1) = 0$). Second, we ignore recovery from early-stage lung cancer to "no cancer" and focus only on cancer progression ($Pr(\theta_{t+1} = 1|\theta_t = 2) = Pr(\theta_{t+1} = 2|\theta_t = 3) = Pr(\theta_{t+1} = 1|\theta_t = 3) = 0$). This implies that treatment for detected early-stage cancer serves only to slow its progression. We define the following probabilities that govern the relevant lung cancer transitions:

- From $\theta_t = 1$:

$$\pi_{12}(h_t, s_t, a_t) = \Pr(\theta_{t+1} = 2 \mid \theta_t = 1, s_t, h_t, a_t) = \text{logit}^{-1}(\alpha_0 + \alpha_1 h_t + \alpha_2 s_t + \alpha_3 a_t + \alpha_4 a_t^2) \tag{9}$$

- From $\theta_t = 2$:

$$Progression: \ \pi_{23}(h_t, s_t, a_t) = \text{logit}^{-1}(\zeta_0 + \zeta_1 \tau_t + \zeta_2 y_t + \zeta_3 (\tau_t \times y_t) + \zeta_4 a_t) \tag{10}$$

$$Stasis: \ \pi_{22}(h_t, s_t, a_t) = 1 - \pi_{23}, \tag{11}$$

where τ_t represents the years since cancer onset ($\tau_t = t - T_i^{\theta_t > 1}$), which we assume is known to an individual

[12] In our preferred specification, we assume that individuals are heterogeneous along two dimensions: their optimism about test quality (captured by high and low subjective beliefs about a test's false positive rate), and the stigma they experience from screening (captured by a high and low additional disutility term from screening). We also consider interaction effects for those who are both pessimistic about test quality and experience stigma costs from screening.

[13] The price of screening depends on the agent's health state and on exogenous health insurance. Because the USPSTF guidelines dictate insurance coverage, we assume that the out-of-pocket price of screening is \$0 if an individual has health insurance and meets the 2021 criteria. We use an price of \$300 per screen for all ineligible screening, which reflects the national average OOP cost (Association et al., 2020).

once diagnosed. As discussed above, diagnosis is a deterministic function of the screening outcomes.

Beliefs at time t ($\tilde{b}_t$) reflect subjective beliefs about any lung cancer at time t. As cancer may progress even without being detected, beliefs about lung cancer are relevant until cancer is diagnosed ($d_t = 1$). That is, if $d_t = 1$, then beliefs are fixed at 1; otherwise, beliefs update differently given the symptom draw, the screening decision, and the results of screening. If the agent chooses not to screen, then the posterior belief of any lung cancer is given as:

$$b_{t+1} = \tilde{b}_t + (1 - \tilde{b}_t)\,\pi_{12},$$

where π_{12} represents the objective transition probability of cancer onset. This says that agents have rational expectations regarding the average evolution of cancer risk. If an agent does not screen, they update beliefs based on these expectations.

If the person chooses to screen and observes a negative signal $z_t = 0$, then uncertainty about θ_{t+1} stems from both the possibility of a false negative test and the average likelihood of transiting to early stage cancer (or remaining there, in the case of a false negative screen). Taking these sources of uncertainty in steps, first, the agent updates beliefs from the negative screening test via Bayes' rule. In this case, beliefs are:

$$\tilde{\tilde{b}}_t = \frac{(1-\rho)\tilde{b}_t}{(1-\rho)\tilde{b}_t + (1-\lambda)(1-\tilde{b}_t)},$$

and now accounting for the fact that cancer may develop by $t + 1$:

$$b_{t+1} = \tilde{\tilde{b}}_t + (1 - \tilde{\tilde{b}}_t)\pi_{12}.$$

If the person chooses to screen and observes $z_t = 1$, then screening has the effect of resolving uncertainty about θ_t, because even a false positive signal generates confirmatory testing. Thus, updated beliefs about θ_{t+1} are the rational expectations of early stage lung cancer in $t + 1$ conditional on the known value of θ_t

$$b_{t+1} = \begin{cases} \pi_{12} & \text{if } \theta_t = 1 \\ 1 & \text{if } \theta_t \geq 2. \end{cases}$$

There is no uncertainty about an individual's smoking history. Define the evolution of deterministic state variables smoking history:

$$h_{t+1} = h_t + s_t, \quad a_{t+1} = a_t + 0.5,$$

where we calibrate the intensive margin of smoking choices to be equal to the median pack-year consumption of a US smoker (0.5 pack-years per year of smoking).

To simplify the other health transition process, we also assume that the other health state $\phi = 2$ is an

absorbing state such that:

$$\Pr(\phi_{t+1} = 2 \mid \phi_t = 2) = 1,$$

and

$$\Pr(\phi_{t+1} = 2 \mid \phi_t = 1, h_t, a_t, s_t) = \text{logit}^{-1}(\psi_0 + \psi_1 s_t + \psi_2 a_t + \psi_3 (s_t \times a_t)). \tag{12}$$

The model also incorporates mortality, the probability of which is increasing in lung cancer and other health states. Note that mortality is not a function of smoking or smoking history; rather, smoking affects mortality indirectly via lung cancer and general health deterioration.

$$\Pr(D_{t+1} = 1 \mid \theta_{t+1}, \phi_{t+1}, a_t) = \text{logit}^{-1}(\omega_0 + \omega_1 \cdot 1[\theta = 2] + \omega_2 \cdot 1[\theta = 3] + \omega_3 \cdot \phi + \omega_4 \cdot a_t) \tag{13}$$

Optimal Behavior. If $d_t = 0$, the agent is unaware of the value of θ, and screening payoff is uncertain. If the agent opts not to screen, then the contribution of current utility to the value function is simply expected utility, $u(\cdot)$, taken over cancer states. This reduces to:

$$\begin{aligned} E(u(x_t = 0, s_t; \Gamma_t)) =& (1 - \tilde{b}_t)\, U_{\theta<3} + \tilde{b}_t \, \frac{U_{\theta<3} + U_{\theta=3}}{2} \\ &+ \frac{(W_t - p_s s_t)^{1-\gamma_0}}{1-\gamma_0} + (\gamma_1 + \gamma_2 h_t + \gamma_3 h_t^2) \cdot s_t - \gamma_6 \mathbb{1}\{\eta_t > 0\}. \end{aligned}$$

With screening, however, expected current utility is the expectation over the likelihood of θ and the (symptom- and screening-updated) beliefs about the quality of the screening test:

$$\begin{aligned} E(u(x_t, s_t; \Gamma_t)) = (1 - \tilde{\tilde{b}}_t) \left[(1 - \hat{\lambda})\, u(x_t, s_t;\, z_t = 0,\, \theta_t = 1) + \hat{\lambda}\, u(x_t, s_t;\, z_t = 1,\, \theta_t = 1) \right] + \\ + \tilde{\tilde{b}}_t \left[(1 - \hat{\rho})\, u(x_t, s_t;\, z_t = 0,\, \theta_t \geq 2) + \hat{\rho}\, u(x_t, s_t;\, z_t = 1,\, \theta_t \geq 2) \right]. \end{aligned}$$

This term is the weighted average of utility over the two possible cancer states (collapsing early- and late-stage cancers) and the signals from symptoms and screening, with weights determined by subjective probabilities both about underlying cancer incidence ($\tilde{\tilde{b}}_t$, defined below) and subjective screening quality ($\hat{\rho}$ and $\hat{\lambda}$).

To close the model, we define the Bellman equation conditional on diagnosis. If $d_t = 0$, contemporaneous θ is uncertain. Then, the value function is the maximum over action space A of the expected value over the

perceived distribution of θ.

$$V(\Gamma_t|\, d_t=0) = \max_{A_t}\Big\{(1-\tilde{b}_t)*(E(u(s_t,x_t;\,\Gamma_t,\theta_t=1))+\beta\mathbb{E}_{\theta,\phi}\left[(1-P(D_{t+1}=1|\,\theta_t=1))V(\Gamma_{t+1}|\,\theta_t=1)\right] + (\tilde{b}_t)*\left[u(s_t,x_t;\,\Gamma_t,\theta_t=2)+\beta\mathbb{E}_{\theta,\phi}\left[(1-P(D_{t+1}=1|\,\theta_t=2))V(\Gamma_{t+1}|\,\theta_t=2)\right]\right]\Big\}. \tag{14}$$

If $d_t = 1$, then θ is known to the agent, screening is irrelevant, and the only remaining decision is whether to smoke. The value function in this case is:

$$V(\Gamma_t|\,\theta_t=3) = \max_{s_t\in\{0,1\}}\Big\{(E(u(s_t,x_t;\,\Gamma_t,\theta_t=3))+\beta\mathbb{E}_{\phi}\left[(1-P(D_{t+1}=1|\,\theta_t=3))V(\Gamma_{t+1}|\,\theta_t=3)\right]\Big\}. \tag{15}$$

Given a finite time horizon, this model can be solved via backward induction to recover optimal screening and smoking behaviors conditional on the set of model parameters, outlined below.

5 Data

Survey

Following a burgeoning economic literature on survey methods (Elías et al., 2019; Ferrario and Stantcheva, 2022; Haaland et al., 2024, 2025), we present results from a novel survey of 4,000 current or former smokers. Our survey ran on the survey research platform Prolific from November 20th, 2025 - February 15th, 2026.[14] Survey respondents come to Prolific and are presented with a set of surveys for which they meet eligibility criteria. Because our interest is in the population at risk for lung cancer, we restrict our eligible survey population to those with some smoking history and who are 40 years of age or older. Our final analysis sample consists of 3,912 respondents.[15]

We begin our survey by asking standard assessments of CRRA risk preferences (Barsky et al., 1997) and time-consistent time preferences (Falk et al., 2018). In both cases, we are able to bound these parameters by classifying respondents based on responses to risk and intertemporal tradeoff questions, respectively. For risk aversion, our survey identifies six categories of respondents ranging from CRRA risk aversion parameters (γ_0) exceeding 7.52 to those less than 0.31. Similarly, for time preferences, our survey identifies eight groups such

[14] Prolific has been used extensively in recent economic research (McGranaghan et al., 2024; Graeber et al., 2024; Augenblick et al., 2025; Exley et al., 2025; Bordalo et al., 2026; Andre et al., 2026).

[15] Appendix Table 1 presents more information on sample construction, and Appendix Table 2 demonstrates that our sample is similar to 2022 Behavioral Risk Factor Surveillance System data in key individual characteristics. The full survey is also available via Qualtrics.

that the time consistent discount factor β ranges from less than 0.476 to greater than 0.943. We then measure health insurance status, income, and residential location at the zip code level. Next, we measure whether the respondent meets the 2021 USPSTF recommendations for LDCT lung cancer screening. Specifically, we ask about current smoking status and age, and we assess a respondent's pack-year smoking history. Whether a respondent is eligible for subsidized screening determines the set of options presented in the randomized experiment that follows.

In the next section, we assess beliefs regarding early lung cancer for a generic person who matches the respondent's age, smoking history, and overall health. We follow this question with an assessment of how different the respondent feels they are from the average matched on these characteristics. Next, we ask respondents about the respondent's history with, and beliefs regarding, LDCT lung cancer screening. These beliefs include subjective assessments of false and true positive rates, as well as assessments of past lung cancer screening. We also ask two questions about perceived stigma, both regarding support from family and about the signal that screening sends about past smoking behavior. We end this section with an assessment of "information avoidance," in which we ask, "If lung cancer screening might bring bad news, I prefer to delay it, even if it's recommended." These questions provide evidence on heterogeneity in beliefs and attitudes regarding screening. Together with basic demographic information provided by Prolific, our baseline information on respondents includes rich measures of smoking and screening history, beliefs regarding lung cancer and screening outcome probabilities, and perceptions of stigma related to screening. We control for variation in these preferences, beliefs, and characteristics in our analysis below.[16]

Table 1 presents summary statistics on the baseline sample, including the count of nonmissing observations, the mean, and three p-values, to be defined below.[17] The mean age of our sample is 52.3; 62% are female; and the percentages of White, Black, and Other races are 82.5%, 7.3%, 10.3%, respectively. Our least risk averse category is defined as having a CRRA γ parameter less than 0.31, which characterizes 5.3% of our sample; the most risk averse group are those with a CRRA γ greater than 7.52, which captures 29% of our sample. Similarly, 37.7% of the sample are in our least patient group, with a discount factor less than 0.476, and 4.1% of the sample have a discount factor greater than 0.941. The sample percentage with no health insurance is 8%, and the income distribution ranging from 16.1% with annual income less than $25,000 and 4% with greater than $200,000 annual income. USPSTF guidelines are based on age, smoking history, and current smoking behavior, and 24.2% of our sample meet all three criteria; 52.7% meet the age criteria, 53% meet the pack-year criteria; and 71.0% are either current or recent smokers.

To gauge beliefs and expectations regarding lung cancer risk, screening quality, and stigma, we ask

[16] See Appendix Figures 1 and 2 for evidence that risk and time preferences are correlated with subjective beliefs and intention to seek screening.

[17] We keep observations with missing baseline information in Table 1, but we drop observations with missing experimental variables. See Appendix Table 1.

respondents the likelihood of early-stage cancer for a person with their age, smoking history, and health characteristics. The mean is 22.17%, and the modal respondent felt that their own risk was similar to the average person's risk. The mean subjective belief that an LDCT lung cancer screen would detect an actual cancer case is 64.37%; and the mean subjective belief of a false positive is 17.9%. We characterized 45.4% of our sample as having "high stigma" surrounding screening, which we defined as the belief that both screening sends a signal about past behavior and that friends and family would be judgmental about seeking a screen. Finally, we asked respondents about information avoidance. In our sample, 17.1% agreed or strongly agreed that they prefer to avoid screening information.

Following the baseline questions, the survey turns to a randomized information experiment, the goal of which is to understand how preferences, beliefs, perceptions regarding screening quality, stigma, and prices shape the demand for lung cancer screening.[18] First, we classify respondents based on whether they meet USPSTF guidelines, and we randomize respondents into four treatment arms: control, stigma, quality, and price. The arms are differentiated by how the intention to screen question is framed. We ask both a 0 to 100 scale question and a binary question, but our focus is on the former.

Arm	**Framing language appended to the common elicitation**
Control (neutral)	None. Respondents receive only the common elicitation stem below.
Stigma reduction	Lung cancer screening is a clinical test like any other. Whether you smoke now or used to, staff are trained to treat every patient with dignity, and screening results are kept private.
Screening quality	Out of every 100 people who get today's standard lung cancer screening (low-dose CT), about 12 will have a false alarm (a positive result when no cancer is present). Most of these are cleared with a repeat scan.
Price — USPSTF eligible	Because of your age and smoking history, the United States Preventive Services Task Force recommends annual lung cancer screening. For most people in your situation, insurance covers the test at no cost to you.
Price — USPSTF ineligible	Because of your age and smoking history, you are not recommended for lung cancer screening under the United States Preventive Services Task Force guidelines. If you choose to receive a screening, most people in your situation pay an out-of-pocket price of about $X.

Notes: Every arm concludes with the common elicitation: "On a scale from 0 to 100, where 0 = definitely will not and 100 = definitely will, how likely are you to seek a lung cancer screening (low-dose CT) in the next 12 months?" In the control arm this stem is presented on its own; in the treatment arms the language shown above is appended (and displayed in italics to respondents). The screening-quality false-positive rate is estimated from our analysis of Truveta EHR data. The price arms are assigned based on USPSTF eligibility, and the out-of-pocket price is randomized over $\$X \in \{100, 300, 500\}$. Each question is followed by a binary yes/no item on lung cancer screening in the next year.

Figure 2: Screening-question framings by treatment arm.

[18] Appendix Section 2 provides a graphical depiction of the experimental design.

After asking the randomly framed screening intention questions, we ask a series of comprehension questions that target understanding about the quality of screening, the process of screening, and the cost. We hypothesize that those receiving the treatment that corresponds to each target should be more likely to agree with our comprehension questions. For example, we ask respondents whether they agree with the statement, "Clinic staff would be nonjudgmental if I asked about screening," which we hypothesize will find more support in those who received the positively framed stigma question. Appendix Figure 3 provides evidence in support of these hypotheses.

Our survey ends with a randomized framing of a question regarding expecting smoking behavior over the following 12 months. The control arm receives the following neutral framing:

> Thinking about the next 12 months, please indicate which option best reflects your expectations regarding your smoking behavior.

In contrast, to capture how smoking behavior may respond to the results of lung cancer screening, the treatment framing adds the following italicized language:

> *Suppose a recent lung cancer screening revealed no evidence of cancer.* Thinking about the next 12 months, please indicate which option best reflects your expectations regarding your smoking behavior.

Importantly, in our intent-to-smoke question, we do not ask respondents to imagine a state of cancer. Here, we are attempting to alleviate uncertainty by presenting a hypothetical clean test result. The goal is to evaluate how intended smoking behavior differs relative to the neutral control framing of the question.

Table 1 presents evidence of experimental balance on three dimensions. The first p-value (p_1) is of the F-test that there are no differences in means between the control arm and the three treatment arms: stigma, quality, and price. The second p-value (p_2) is on the F-test of no differences in means between the lowest price treatment ($100) and the other two prices ($300 and $500), conditional on being randomized to the price arm and being ineligible for free screening. The final p-value (p_3) is on the t-test that there is no difference in means between the treatment and control arm of the smoking experiment. We find very little evidence, beyond what would be expected randomly, of statistically significant differences across treatment arms. Nevertheless, we control for baseline characteristics in Table 1 in our analysis of the treatment effects.[19]

Our main regression equation relates Y_i, the measure of intention to screen, to binary variables for our

[19]Rather than drop observations, we record the small number of missing values of our control variables and control for these recoded observations.

treatment arms and the baseline characteristics:

$$Y_i = \alpha + \beta_S 1\{\text{Stigma}\} + \beta_Q 1\{\text{Quality}\} + \sum_j \Big(\beta_P 1\{\text{Price=j}\} \cdot 1\{\text{Ineligible}\}\Big) + \beta_{PE}\, 1\{\text{Eligibility Information}\} \cdot 1\{\text{Eligible}\} + \mathbf{X}_i'\boldsymbol{\gamma} + \varepsilon_i, \tag{16}$$

where $j \in \{\$100, \$300, \$500\}$. Here, coefficients β_S and β_Q reflect treatment effects of the stigma and quality treatment arms, relative to the control arm, and β_P and β_{PE} represent treatment effects of the price arm those who do and do not meet the USPSTF guidelines, respectively.

Figure 3 presents estimates of the treatment effects in Equation 16, along with robust, 95% confidence intervals. Relative to the control mean of 38.25, the intention to screen is 10.2% higher in the stigma arm, but it is not significantly different in the quality information arm. Conditional on USPSTF eligibility, information about screening coverage increases intention to screen by 40%. For those who do not meet the guidelines, intention to screen falls by 16.2%, 33.7%, and 41.1% for price quotes of \$100, \$300, \$500, respectively, relative to the control arm. A feature of our experiment is that comparing treatment effects within those randomized to the price arm separately identifies the effect of prices from the effects of learning about USPSTF guidelines. Indeed, focusing on ineligible respondents receiving a price quote, we calculate an average extensive margin participation elasticity of -0.17.

Next, we assess heterogeneity in treatments effects. Specifically, we hypothesize larger effects of the positive stigma framing among those who, at baseline, admit to feeling stigma. Relative to the control mean, the effect of the positive stigma information is 13.0% among those classified as having high stigma at baseline. For those with low baseline stigma, the effect is smaller at 7.9%.

Our quality framing presents the true false positive rate of screening of 12%; for respondents whose baseline, subjective assessment of the false positive rate is higher, our treatment represents "good" quality news, and we expect that our quality treatment should encourage screening. Similarly, for respondents whose baseline, subjective assessment of the false positive rate is lower than 12%, our treatment reflects "bad" news. Allowing the quality information treatment effect to vary by baseline beliefs, we see that "bad" news respondents in this arm are less likely to screen, and "good" news respondents are more likely to screen, but neither effect is statistically significant. Finally, we assess heterogeneity in the price effects by income, allowing the price treatment effects to vary by whether the respondent reports more or less than \$50,000 in annual income. Here, we do not find significantly different treatment effects, even as we are controlling for other socioeconomic characteristics, including health insurance status.

Finally, we evaluate treatment effects from our smoking experiment by focusing on the subset of respondents who claim to be currently smoking at baseline, and we model how their intention to quit smoking varies by our "clean scan" treatment. Define $Q_i = 1$ if the respondent selected "I will completely quit smoking,"

and 0 otherwise. We estimate:

$$Q_i = \beta_0 + \beta_1 1\{\text{Treatment}\} + \mathbf{X}_i'\boldsymbol{\gamma} + \epsilon_i, \tag{17}$$

where β_1 is our coefficient of interest. Figure 5 presents estimates and robust confidence intervals of β_1, both overall and across several subgroups of interest. The control mean of intention to quit among our 1,342 current smokers is 0.216. Overall, intention to quit smoking is 16.7% higher in the treatment group. Next, we allow for heterogeneity in the treatment effect by time preference. We define "more patient" and "more impatient" groups based on whether the time consistent discount factor is more or less than 0.5. The more patient group constitutes 38.57% of our sample. The "clean scan" treatment is larger for the more patient group (27.8%). We also find a much larger treatment effect (0.114 vs. 0.027) in those without insurance, although these results are imprecise. We find a large and statistically significant increase in intention to quit (29.6%) for those who had never received a lung cancer screening. Finally, we find the largest treatment effect on those who assessed their own risk as "much higher than average."

Truveta

Truveta compiles and standardizes daily electronic health record (EHR) data from over 130 million patients, representing 100 health systems across the United States. The Truveta data provide longitudinal, patient-level clinical information, including diagnoses, procedures, imaging utilization, and follow-up care. Indeed, for patients who seek care in different systems within Truveta coverage, we are able to link standardized records across providers and payers. We use Truveta to measure real-world screening outcomes and diagnostic pathways. These data are particularly well suited to our setting because they allow us to observe the full sequence of events surrounding lung cancer screening, including initial low-dose CT (LDCT) scans, subsequent diagnostic testing, and confirmed cancer diagnoses. Our primary use of the Truveta data is to identify objective screening test characteristics and diagnostic outcomes. In particular, we estimate rates of false positives and follow-up testing conditional on screening, as well as the distribution of diagnostic resolution after an initial positive screen.

Within the Truveta environment, we define a population of individuals who have ever either had an LDCT lung cancer screening or been diagnosed with lung cancer. Of this 4.8 million individual population, we take a 1.5% sample, representing 72,000 patients and 17 million medical encounters. Over 95% of our sample are above the age of 31; 71.8% are white, 48.1% are male; and the modal group, representing more than 43,000 patients, are observed in over 61 medical encounters over at least 15 years.

Within our sample, we observe 264,000 initial, LDCT lung cancer screens. Figure 6 presents a flow diagram of the outcomes. Following the initial screen, we define a category of any confirmatory testing within the

subsequent three months. In our sample, 14% had confirmatory testing within three months. Next, we define a binary variable of any cancer diagnosis within 12 months of the initial screening. Of those with confirmatory testing, 88% had no cancer diagnosis within 12 months, and, of those with no confirmatory at three months, 99% had received no cancer diagnosis at 12 months. We base our definition of a "false positive" from the diagnosis indicator. Specifically, of the 264,000 initial screens, 259,000 had not resulted in a cancer diagnosis. However, the 12.5% (33,000) who received confirmatory testing likely received something other than a "no cancer" result from the initial screen. The ratio of these counts yields a false positive rate of 12.7%.

National Lung Screening Trial

We use data from the National Lung Screening Trial (NLST) to identify policy-invariant health transition parameters. The NLST enrolled over 50,000 high-risk individuals with substantial smoking histories and randomly assigned them to LDCT screening or chest radiography, generating experimental variation in screening exposure and subsequent health outcomes. The trial provides detailed information on cancer incidence, stage at diagnosis, disease progression, and mortality over up to 7 years.

We use the NLST to estimate two policy-invariant transition parameters that govern the biological evolution of disease in the absence of endogenous behavioral responses: (i) the onset of early-stage lung cancer among individuals who are currently cancer-free, and (ii) the progression hazard from early-stage to advanced disease. Because screening assignment is randomized, these estimates are not confounded by selection into screening and therefore provide a natural benchmark for disease dynamics, which we treat as fixed inputs in the structural estimation.

Onset of early-stage cancer. We first model the transition from cancer-free to early-stage disease. Restricting the sample to individuals observed to be cancer-free at baseline (denoted $\mathrm{N}_i = 1$), let $\mathrm{Onset}_i = 1$ indicate a transition into early-stage lung cancer in the subsequent period. We model this transition as

$$\Pr(\mathrm{Onset}_i = 1 \,|\, \mathrm{N}_i = 1) = \Lambda\Big(\alpha_0 + \alpha_1 h_i + \alpha_2 s_i + \alpha_3 a_i + \alpha_4 a_i^2\Big)\,, \tag{18}$$

where $\Lambda(\cdot)$ is the logistic CDF, s_i is an indicator for current smoking, h_i is cumulative smoking history (pack-years, measured in 10-pack-year increments), and a_i is age (measured in decades over age 40). We estimate (18) by maximum likelihood with heteroskedasticity-robust standard errors. To summarize the estimated onset surface, we compute average predicted onset probabilities over the empirically relevant ranges of smoking history (pack-years from 30 to 90) and age (55 to 74). These predicted probabilities constitute the cancer-free $\rightarrow$ early-stage transition rates used to calibrate the model. Appendix Table 3 provides estimates and standard errors of the α parameters that dictate early-stage cancer onset and the π parameters that dictate

cancer progression. Appendix Figures 4 and 5 show the margins plots of early-stage onset by pack-years and age, respectively. In the first wave, we observe 43 early-stage cancers out of the 19,061 individuals who are confirmed to be cancer free in the previous wave (i.e., baseline). Throughout the NLST, we observe 101 cancer progressions of the 1,876 early-stage cancer cases.

Progression conditional on early-stage disease. We next estimate the rate at which early-stage disease progresses. We restrict the sample to individuals with confirmed early-stage lung cancer ($\text{stage_grp}_i = 1$ and $\text{conflc}_i = 1$) and re-center the time axis at the onset of early-stage disease: subtracting each individual's cancer-free duration d_i from both the time of first progression and the last progression-free observation makes the clock start when early-stage disease is established rather than at enrollment. Let T_i denote time (in years) from early-stage onset to progression; individuals never observed to progress contribute right-censored durations at their last progression-free observation, and observations with undefined event times are dropped. We discretize follow-up into annual intervals $\tau \in \{1, \ldots, 7\}$ and let $D_{i\tau} = 1$ indicate progression of individual i during interval τ. The discrete-time progression hazard is

$$\lambda_i(\tau) = \Pr(D_{i\tau} = 1 \,|\, T_i \geq \tau) = \Lambda(\zeta_0 + \zeta_1 \tau + \zeta_2 y_i + \zeta_3 \,(\tau \times y_i) + \zeta_4 \, a_i)\,, \tag{19}$$

where y_i indicates receipt of lung-cancer treatment. We estimate (19) as a pooled logit over person-period observations formed by episode-splitting each individual's follow-up at every year $\tau = 1, \ldots, 7$, with standard errors clustered at the individual level. The coefficient ζ_1 captures duration dependence in the progression hazard, ζ_2 the level shift associated with treatment, and ζ_3 whether treatment alters the time profile of progression. Together with the survival estimates, the onset and progression parameters in (18)–(19) constitute the fixed health-transition inputs used in estimation.

Behavioral Risk Factor Surveillance System

We use data from the 2022 Behavioral Risk Factor Surveillance System (BRFSS), a large, nationally representative survey of U.S. adults, to generate empirical moments on smoking behavior and screening prevalence among US adults with a positive smoking history. The BRFSS provides detailed information on smoking status, smoking history (including pack-years), demographics, and self-reported health, as well as information on preventive care utilization. The 2022 wave of BRFSS data includes detailed information on lung cancer screening, including screening history and screening outcomes. We restrict the sample to individuals with a history of smoking and construct age-specific profiles of smoking and screening behavior that are comparable to the population targeted in our model and experimental data.

Data from the 2022 BRFSS provides externally valid moments on the distribution and dynamics of smoking

behavior over the life cycle, which we use to discipline preference parameters governing addiction and habit formation. We restrict attention to the 116,709 observations (of 444,685) for respondents between the ages of 40-80 who have some smoking history. Appendix Table 3 presents survey weighted estimates of linear probability models of cigarette smoking on the count of pack-years of smoking history and its square. These parameters reveal a concave relationship between the probability of smoking and smoking history, and they are in line with the policy invariant parameters recovered in Darden (2017). Appendix Figure 6 shows this relationship over the support of pack-years of smoking history.

We also use BRFSS data to demonstrate how screening prevalence evolves over the age profile. In a subsample who meet the criteria above and who have non-missing values of the screening questions, Appendix Figure 7 demonstrates screening prevalence for two groups. First, we plot screening prevalence among individuals who otherwise qualify for subsidized screening under the 2021 USPSTF guidelines. For these individuals, those who have 20 or more pack-years of history and who are current or recent smokers, the age 50 threshold triggers subsidized screening. The second group includes those who do not meet the pack-year and/or current smoking requirements (but who still have some smoking history). The figure clearly demonstrates an increase in screening at age 50 for the first group.

Other Health and Mortality Evidence

For health outcomes other than lung cancer, we identify model parameters using external, condition-specific risk tables for cardiovascular disease, chronic obstructive pulmonary disease, and selected non-lung cancers. These tables are used to estimate the age-, sex-, and smoking-status–specific contribution of competing health risks not explicitly modeled as lung cancer outcomes. For cancer outcomes outside lung cancer, we use risk-estimation resources such as the National Cancer Institute colorectal cancer risk calculator, which estimates absolute colorectal cancer risk from demographic, medical-history, family-history, lifestyle, and cigarette-use inputs. The calculator specifically incorporates cigarette-use history, including ever-smoking status, age at smoking initiation, current smoking status, age at cessation, and cigarettes smoked per day, making it a useful external reference for calibrating smoking-related non-lung-cancer risk parameters.

Mortality parameters are calibrated from population-based life expectancy and cancer-survival data. Baseline all-cause mortality is anchored to life tables, including SEER expected-survival life tables, which are generated from U.S. mortality data and provide conditional survival probabilities by age, sex, calendar year, and race/ethnicity group. Cancer-specific mortality and survival inputs are informed by SEER data, an authoritative U.S. source for population-based cancer statistics, including incidence, survival, and mortality information. We further adjust mortality assumptions for comorbidity using published evidence on the effect of chronic disease burden on life expectancy, including recent longitudinal evidence on the additive impact of COPD and cardiovascular disease on all-cause and disease-specific mortality. Together, these sources allow

the model to reflect both background population mortality and excess mortality associated with cancer and chronic cardiopulmonary comorbidity.

Reduced-Form Evidence

Our randomized information experiment yields three findings. First, price effects dominate other behavioral mechanisms; informing USPSTF recommended respondents of their eligibility for free screening increases intention-to-screen by 40%, whereas informing respondents of the 12% rate of false positives identified in Truveta EHR data does not change behavior on average.[20] Second, baseline heterogeneity in beliefs and stigma interact with treatment to drive behavior. For example, for those respondents exhibiting some stigma associate with screening at baseline, there was a significant effect of information targeting these beliefs on screening intention. Finally, we find no evidence of moral hazard. Being informed of a clean screening result increases the intention to quit smoking among current smokers by 16.7%, an effect that is driven by time preferences, screening history, and self-assessed risk perceptions.

6 Model Estimation

Moments & Estimation

We estimate the equilibrium model parameters using simulated GMM, matching observed moments from our experimental and clinical data to simulated moments in the model. As our model is based on a combination of multiple unique data sources, we estimate the model on a simulated dataset of 1 million smokers, whose characteristics are calibrated to be representative of the BRFSS and experimental data. In each step of solving the model, for a given guess of the model parameters (Θ_0, defined below), we solve the full model by backward induction, allowing agents' health, beliefs, and utilities to evolve over time as defined above. Solving the model in this way is feasible, as agents have a finite lifespan and make only two binary choices in each period (smoking and screening). Doing so yields estimates of the optimal smoking and screening decisions across the entire state space, meaning for all agents conditional on their demographics, smoking history, and health; it also allows us to compute the selected moments. We then iterate over this approach until the observed and simulated moments converge to identify Θ^*.

In estimation, we use moment conditions capturing (i) age-specific smoking prevalence, (ii) the relationship between smoking and cumulative smoking history, (iii) screening rates by eligibility status, and (iv) our experimentally identified responses of screening to price, stigma, and perceived test quality. Table 2 defines

[20] Our data suggest the false positive rate is 12.7%, but there is considerable variance in the literature (Aberle et al., 2011; Pinsky et al., 2013; de Koning et al., 2020; Pinsky et al., 2015).

all moments used in estimation. First, we target age profiles of smoking by matching mean smoking rates across age bins observed in the BRFSS data for those with smoking history by age 40. Second, we match the relationship between smoking and cumulative smoking history (pack-years), including both levels and slopes, to capture persistence and reinforcement in smoking behavior over the life cycle (Becker and Murphy, 1988). Third, we match average screening rates separately for individuals above and below each USPSTF eligibility threshold, capturing those who opt into screening as they cross one threshold but not another (Darden and Hoagland, 2025). Fourth, we use experimental variation to discipline how screening responds to prices, stigma-related barriers, and perceived test quality. Fifth, we use SEER survival data and the subjective beliefs elicited by our survey to pin down the trajectories of cancer and chronic health onset and belief evolution.

GMM estimation allows us to recover key model parameters governing selection into screening, smoking, and belief evolution. Other parameters, such as those governing risk aversion, time discounting, and health transitions, are fixed in our model based on prior literature and our own first stage estimates using claims data. This approach reduces the state space for Θ^* and makes solving the model tractable. Table 3 summarizes all parameters defined in Section 4 that are calibrated, as well as the calibrated value, its source, and bounds on the value used in assessing model stability.

Machine-Learning-Assisted Initialization for Structural GMM

Estimating structural models by GMM often requires solving a difficult, non-convex optimization problem. In such settings, convergence and equilibrium parameter vectors can be highly sensitive to the initial starting point. We therefore implement a machine-learning (ML)-assisted warm-start procedure designed to deliver starting values that are both computationally efficient and economically plausible. The procedure preserves the conventional structural GMM estimator while incorporating ML algorithms to guide the choice of initial conditions.

The algorithm proceeds in three steps. First, we perform a grid search, in which we draw 25,000 candidate parameter vectors using a Latin hypercube design over the admissible parameter space. For each candidate, we solve the structural model, simulate a cohort, and compute the vector of average model-implied moments. We also generate a binary indicator for whether the candidate vector implied a corner solution (e.g., no smoking or no screening). Second, using the simulated moments as training data, we estimate a separate XGBoost regression for each moment and an XGBoost classifier for whether the candidate vector resulted in a corner solution. The moment-specific regressions produce a flexible approximation to the mapping from structural parameters to model moments, while the classifier estimates the probability a candidate start lies in a region leading to a corner solution. Because the regressions are fit moment by moment, the procedure can accommodate heterogeneity in predictability across moments (e.g., an optimal weighting matrix from a

previous iteration). Finally, we generate a much larger set of unevaluated candidate parameter vectors and use the trained models to predict their implied moments and corner-solution probabilities.[21] This results in a small set of optimal starting vectors, which can be used for the actual structural estimation and to evaluate model stability relative to distinct starting values.[22]

A novel part of the grid search is that for each candidate, we compute an indicator for whether the simulated behavior is effectively at a corner solution. That is, for a given starting vector, we simulate the model and assign a flag if the implied smoking or screening rates are near zero or one. This classification step is important because some regions of the parameter space generate behavior that is numerically admissible but economically uninformative for local optimization. Such regions can trap gradient-free or local-search routines in parts of the parameter space that are unlikely to yield an empirically credible interior fit. The corner indicator is used only in the warm-start stage; in the main structural estimation, we do not constrain the predicted smoking or screening behaviors in any way. Hence, this requirement can be flexibly implemented across many GMM routines in different ways, as it is not used as a target moment in the resulting GMM estimation. Instead, this condition could be flexibly adapted to many circumstances where certain properties of a starting vector are more or less desirable.

Our approach to using ML-assisted techniques to identify a warm start to standard GMM optimization is novel, but related to several important developments in structural estimation. Some work in this area has relied on ML to learn the relationship between moments and parameters directly, particularly for simulated estimation techniques (Catherine and Ebrahimian, 2024; Duarte and Fonseca, 2023). These papers use supervised learning to exploit the geometry of a model-implied moment surface, but they ultimately replace the structural estimation routine itself. We, on the other hand, leave in place the conventional GMM estimator and use ML approaches in a conservative way only to improve the starting parameter vector. Our approach also allows for ML selection of weights on moments, complementary to recent work using ML to automate moment selection (Zila and Kukacka, 2023). While this work empirically selects moments, we continue to prioritize theoretically-selected moments while learning from the data the best weighted objective function to apply across those moments. Our approach is especially useful in applications where solving the model is costly, the objective is irregular, and poor starts frequently lead to local minima or economically degenerate solutions.

[21] These predictions are generated using a criterion mirroring the objective used in estimation. Specifically, we use the optimal weighting matrix to combine individual moment predictions, but trim extreme eigenvalues to maintain numerical stability. We additionally include a dispersion penalty based on the cross-moment standard deviation of the predicted values to exclude starting values with extremely poor predictions in one or more moment dimensions.

[22] As a robustness check, we also perform simulated annealing as an optimization method for our starting points, to verify that the optimizer is not routinely converging to local, rather than global, optima.

Model Fit & Key Results

Table 4 presents the main estimates for the model parameters, including a brief discussion of their individual identification. In this section, we discuss the overall fit of the model to the moments discussed in Table 2 and the key implications of the model estimates.

The estimated model provides a good fit to a large number of statistics from our various data sources, including smoking and screening rates from the BRFSS data and our experimental results. In particular, we verify that the equilibrium model prediction validates the experimental evidence presented above: the model generates strong price effects as well as responses to changes in an individual's optimism or stigma for screening. Here, we highlight three key implications validated by our model; additional results are presented in the Appendix.

Price Sensitivity in Screening Decisions. First, the model implies that screening decisions are highly price sensitive, but that screening also happens frequently outside of the USPSTF eligibility thresholds (Darden and Hoagland, 2025). Figure 7 shows both empirically observed and predicted screening rates stratified by both age and smoking history. The figure highlights two facts: first, nearly half (48.6%) of all LCS screening happens when individuals choose to pay out of pocket for a screening. A substantial portion of this screening (28% of all screening) occurs even for individuals who meet neither of the relevant thresholds. Second, screening rates increase when the price drops (for example, when individuals in the high smoking-history group pass the age 50 cutoff in the second panel of Figure 7). The preliminary model matches the qualitative increases in screening around eligibility thresholds and the relative ranking of screening rates by age and smoking history.

Individuals choosing to pay for screening are informative about the relative value of screening, as discussed above. Screening is triggered in the model when subjective beliefs about cancer risk rise, driven by signals from smoking, health transitions, or symptoms. Based on the estimated model parameters, when individuals face the full price of screening (roughly $300), they choose to screen when their beliefs about cancer risk are 28.0% or higher. After meeting USPSTF eligibility requirements, this threshold drops by roughly one third to 19.5%.

Effects of Screening on Future Health Behaviors. Second, the model fit also highlights how screening affects future investments in preventive health, such as an individual's decision to continue or cease smoking. As discussed in Section 2, the value of screening complements prevention based on three sufficient statistics, which we can now estimate directly in our context. First, addiction should not be so large as to restrict a behavioral response to screening. In our model, we observe two pieces of evidence supporting this hypothesis. First, we observe sharp elasticities for screening and smoking with respect to price, suggesting that health

behaviors are not fully inelastic. Second, as shown in Table 4, the relative value of being in the good state of the world (measured by $U_{\theta<3}$) is roughly 5.7 times the utility from smoking even with significant smoking history (e.g., when evaluated at $h_t = 20$). The second sufficient statistic, which is that the test be informative, is met both in theory and in subjective expectation, as individuals in the survey and in the model consider a lung cancer screen to convey information about true underlying health. Finally, the framework requires that the state-specific return to prevention in the good state of the world be larger than in the bad state in order for the value of life effect to dominate the moral hazard effect ($\delta_B - \delta_G < 0$). This condition follows directly from the returns to quitting smoking in the model. Equation (13), capturing mortality effects, does not depend on smoking or smoking history directly, meaning that once an individual has late-stage cancer, smoking cessation delivers essentially no survival gain ($\delta_B \approx 0$). On the other hand, consistent with the epidemiological evidence presented above, smoking cessation lowers both the hazard of lung cancer incidence and the onset of chronic conditions when an individual does not have late-stage cancer (so that $\delta_G > 0$). Simulating the model, we find that a marginal increase in cessation raises one-year survival by 2.0 percentage points among those with no or early-stage cancer, compared to 0.15 percentage points among those with late-stage disease, consistent with this fact.

Overall, then, the model estimates directly imply that the continuation of life effect should dominate any moral hazard effects, meaning that we should expect screening to complement prevention (in this case, smoking cessation). Given the additional structure afforded us by the model in Section 4, we can directly estimate the relationship between a first screening and future smoking decisions to validate this finding.

To do so, we use the simulated data under the equilibrium model parameters—which govern endogenous selection into screening—and run a stacked difference-in-differences model comparing the evolution of smoking behavior for current smokers who screen for the first time to a set of clean controls (Wing et al., 2024). That is, we define a set of sub-experiments (indexed by d) for each 1-year age group; for each experiment, we compare a treatment group of those who smoke continuously for at least five years and then screen in year d to a comparison group of 5-year smokers who will not screen for the first time until at least $d + 5$. We then stack each sub-experiment and run a standard dynamic difference in differences estimator:

$$Y_{it}^d = \sum_{k=-5,\neq -1}^{5} \beta_k \left(\mathbb{1}[t - E_i = k] \times \text{treated}_i^d \right) + \alpha_i^d + \alpha_t^d + \varepsilon_{it}^d \tag{20}$$

where $t - E_i$ indicates years relative to first screening event time, and we adjust for individual and time fixed effects within sub-experiments. We cluster standard errors at the experiment level and report results relative to the year prior to screening.

In the population-level data implied by the model, we first observe that screening is associated with an 8.4 percentage point reduction in smoking, corresponding to a 25.5% drop from the baseline smoking rate. This response is consistent with a value-of-life channel in which favorable health information increases the

return to preserving future health and matches the experimental evidence presented above.

Figure 8 presents the results from estimating the dynamic version of this regression for those who smoke prior to their first screening (Equation 20). In the year of screening, the likelihood of continued smoking drops by 10 percent relative to clean controls. Over the following five years, smoking declines by an average of 25 percent, in keeping with the population-level results.[23]

We also consider the robustness of this result to various modeling choices, paying particular attention to the choice of calibrated parameter values. Appendix Figure 9 shows how the estimated (pooled) coefficient from the stacked DD approach varies across models with different values for these calibrated parameters. In this figure, we iteratively vary a single calibrated parameter using the bounds in Table 3, re-solve the model and run the stacked DD design, and then collect the results into a single histogram. The results indicate consistent negative effects of screening on future smoking, precisely estimated in each specification.

Taken together, these results indicate strong value-of-life effects that dominate any potential for moral hazard effects.

Alternative Drivers of Screening and Smoking. Third, the model allows us to consider how selection into screening and smoking is endogenously driven by one's own lifetime survival risk and type. Figure 9 stratifies screening and smoking decisions by those who die before age 70 versus those who survive. Individuals who die earlier are consistently more likely to smoke, consistent with prior work. Interestingly, however, we observe little difference in the rate of taking up screening across these two groups. If anything, those who survive to age 70 are slightly more likely to select into screening. In general, however, we observe little difference in cumulative lifetime risk driving screening decisions.

The equilibrium model parameters also give a sense of the relative importance of each of the mechanisms we study, including the relative roles of prices, beliefs, stigma, and optimism about test quality in driving screening takeup and subsequent smoking decisions. While the model fits the requisite moments well (e.g., identifying a price effect when an individual becomes eligible for free screening), it is generally agnostic about the relative importance of each channel, making this an interesting equilibrium exercise.

As a benchmark, one can compare estimated utility losses from screening under various states to the utility loss from symptoms. Without taking into account price, optimism, or stigma effects, the estimated utility losses from screening are roughly 1.25 times the utility losses from symptoms. Interestingly, the utility effects of pessimism about test quality and stigma from receiving a screening diverge meaningfully: screening disutility for an individual with low confidence in screening is roughly 14.5 times larger than general screening

[23] In Appendix Figure 8, we include simulation results underscoring that this result isn't merely an artifact of the calibrated model. In this simulation, we maintain the preferred values of the calibrated parameters, but perturb the equilibrium parameters values in such a way to bias the model results in favor of a stronger moral hazard effect. The resulting event study highlights that under plausible parameter value choices, it would have been possible to obtain a result where screening incentivizes future smoking rather than encouraging it, in line with the sufficient statistics approach outlined in Section 2.

or symptom disutility, while screening disutility from stigma effects are much smaller, and more comparable to general screening disutility.[24] This is intuitive, as it indicates that optimism about screening—which directly influences how screening modifies individual beliefs—is a more powerful driver of screening decisions than a factor merely influencing the extensive margin of screening (stigma). This is particularly true once screening becomes free.

7 Counterfactual Simulations

Given the estimated model, we are now able to answer key questions related to the value of screening when screening and health behaviors are endogenously correlated. In this section, we present the results of two key counterfactuals. First, we examine the value of a negative screen even for low-risk individuals, by highlighting the effects of exogenous, universal screening at age 45. Second, we explore counterfactual simulations that attempt to induce this screening by varying the price of screening, USPSTF eligibility, and targeting individuals with high stigma or pessimism about a test.

First, we assess how negative LC screening, even for individuals with relatively little *ex-ante* cancer risk, may affect lifetime trajectories of smoking, cancer incidence, and mortality. We do this by imposing a counterfactual policy meant to exogenously provide information on cancer risk, and then assess the extent to which this generates continuation value effects that outweigh any potential moral hazard effects. That is, we assume universal screening for all individuals with any smoking history at age 45 and examine how this induces individuals to quit smoking, as well as any downstream effects this has on cancer development and progression and mortality.

Figure 10 presents the results. We find that imposing a one-time universal screen for smokers at age 45 results in individuals quitting smoking 11.9% of the time; conditional on being a current smoker at age 44, this jumps to 51.4%. For this sample, the average quitter goes an additional 7.5 years without smoking compared to baseline. Not all of this cessation is permanent; we estimate that by age 65, only about one third of those who quit smoking at age 45 are still not smoking. However, smoking reductions still extend the number of cancer-free years for 16% of quitting smokers (8.2% of all who smoke at age 44), with an average of 4.0 additional cancer-free years. This constitutes a 2.2% decline in lung cancer incidence in this population. This directly translates to improved longevity: conditional on reduced cancer incidence, 80.2% experience longer life, with an average gain of 7.9 years.

Taken together, these results imply that even universal screening for an overall low-risk population can improve health behaviors and generate real returns on cancer development, progression, and mortality. With that in mind, a natural question is whether policy levers such as eligibility criteria or cost-sharing can mean-

[24] We also estimate an interesting interaction effect, where individuals facing high stigma and pessimism about screening quality incur additional utility losses roughly equivalent to the baseline utility loss from stigma.

ingfully induce screening. We therefore present the results of a second set of simulations, where we vary these policy levers and measure whether screening was induced, and how much other outcomes changed as a result.

Table 5 presents the results. Offering screening at no cost to anyone with a history of smoking dramatically increases screening takeup and increases overall lifetime utility among all age-40 smokers by 4.9%. Eliminating prices induces over a one third reduction in smoking years, ultimately increasing cancer free time for 5.9% of the population. One can calibrate these estimates based on their preferred value of remaining life at age 40. Two plausible estimates here include the inflation-adjusted figure used by Murphy and Topel (2006) of $10.77 million, and the value of $12.26 million used by the EPA (U.S. Environmental Protection Agency, 2026), both measured in 2026 USD. Scaling our estimates by these values corresponds to a range of $527,730 to $600,740 in additional value of life experienced per person, averaged across all individuals with any smoking history at age 40. Throughout, we report both percentage increases and these scaled estimates; the results we present can therefore be easily scaled by a different value of life parameter if desired.[25]

These health effects are therefore significant – if one considers that the average cohort of 40-year old US citizens is approximately 4.4 million and around 27.5% of that cohort has any smoking history, a plausible range for the total value of eliminating screening prices is between $638.6 billion and $726.9 billion per cohort. Importantly, more targeted policy interventions can also yield significant gains at lower cost. Table 5 indicates that extending eligibility for USPSTF-covered screenings along either dimension also generates meaningful smoking cessation, cancer prevention, and longevity. Moving eligibility from 50 years old to 45 does relatively little to increase screening and influence downstream behaviors, potentially due to the short nature of this shift. By contrast, allowing smokers with moderate smoking history (10 pack-years) free screening causes large increases in screening (60.7%) and corresponding reductions in smoking (12.1%), cancer onset (2.0%), and utility (0.56%). We estimate that 73.1% of smokers would benefit from this policy and put the average lifetime gain across all those with smoking history in the range of $60,312 to $68,656 per person, or between $73.0 billion and $83.1 billion per cohort.

This pattern is plausible, given that the value of a negative screen is likely maximized for individuals under the age of 50. It has generally been established that when an individual ceases to smoke before age 50, the subsequent risk of lung cancer is greatly reduced as lung tissue is most likely to recover (Yoshida et al., 2020). Hence, if negative screening induces smoking cessation due to the continuation-of-life effect, health effects will be maximized for screens that are incentivized for those under the age of 50. This is more effectively done by relaxing the USPSTF eligibility thresholds, rather than more sweeping reforms or relying on individual type changes.

[25] These counterfactual simulations and their corresponding changes in lifetime expected utility are related to the numerator of a typical marginal value of public funds (MVPF) calculation, where the MVPF reflects the ratio of aggregate beneficiary willingness to pay to the net cost borne by the government (Hendren and Sprung-Keyser, 2020).

Decomposing Welfare Gains

These counterfactual simulations, and their corresponding welfare estimates, capture the expected change in discounted lifetime value under the counterfactual and baseline price schedules. That is, for each simulated individual i, we let V_i^1 and V_i^0 denote expected discounted lifetime value under the counterfactual and baseline price schedules, and then integrate over the stochastic evolution of symptoms, disease, and behavior to calculate the lifetime differences in utility given by:

$$\Delta V_i \;=\; V_i^1 - V_i^0 \;=\; \mathbb{E}_{40}\left[\sum_t \beta^{\,t-40}\, S_{it}\left(u_{it}^1 - u_{it}^0\right)\right], \tag{21}$$

where S_{it} is the survival probability to age t. Because screening eligibility is realized only for those who both smoke and survive for sufficient time, ΔV_i gives us the *ex-ante* valuation of the policy. This is the policy-relevant object for evaluating a policy at baseline, when the rule is announced.

Importantly, ΔV_i is an equilibrium object derived under optimal behavior, so it encompasses the value of smoking cessation as well as utility gains from longevity, and the disutility of additional screening. Our model allows us to decompose these welfare gains to isolate those which are specific to changes in health behaviors. In the model, increased screening can generate lifetime utility gains through quitting, which raises the expected value of longer and healthier life-years; it also can generate more mechanical shifts in utility through improved detection, earlier treatment, and reduced healthcare costs downstream. Estimating how the value of improved screening eligibility depends on endogenous health behaviors is essential to correctly value these policies relative to their costs.

To isolate the gains from changes in prevention, we apply counterfactual simulations in stages, holding health behaviors fixed in an intermediate step to isolate their effects on utility. That is, we estimate an intermediate version of the model where the counterfactual policy (e.g., changes in screening eligibility from age 50 to 45) affects screening choices, but where smoking choices are fixed at their baseline levels. Utility changes for the counterfactual policy in this world, relative to baseline, capture the fraction of total lifetime utility gains which are *independent* of changes in health behaviors. The object of interest is therefore the residual, which captures how changes in smoking affect lifetime utility.[26]

The results from this approach suggest that a meaningful fraction of utility gains for expanded screening eligibility comes from changes in health behaviors. When expanding eligibility from age 50 to age 45, 17.8% of gains stem from changes in smoking behavior. Similarly, changes in smoking behavior account for 20.9% of gains for a policy expanding eligibility from 20 pack-years to 10. This corresponds to between $12,605 and $14,349 per person.

[26] This residual reflects differences in utility through the increased value from additional life-years as well as the balance of years spent healthy, in addition to utility gains from reduced spending on cigarettes and future cancer treatments.

Taken together, these results indicate even small expansions in screening eligibility may generate significant differences in quitting smoking and improve welfare. Considering the endogenous relationship between screening and prevention provides important nuance into how these policies should be valued and potentially implemented, as changes in smoking can account for as much as one fifth of overall welfare effects.

8 Conclusions

This paper studies screening as an endogenous information technology whose value depends on the behavioral response it induces. This is common when healthcare services, such as screening, are more effective when combined with preventive health behaviors. We write a dynamic model in the context of lung cancer screening, where individuals choose whether to acquire information about latent cancer risk while also choosing whether to continue smoking, the primary behavior that generates that risk. We estimate the model by relying on a randomized information experiment with clinical records, trial evidence, and nationally representative survey data. In estimating and evaluating the model, we show that screening cannot be evaluated independently of other health investments. Screening demand is highly price sensitive, but selection into screening is not governed by price alone: subjective risk beliefs, stigma, and perceived test quality all shape who screens and when. The model rationalizes substantial screening outside USPSTF eligibility thresholds, even as many eligible individuals remain unscreened, and it implies that marginal screeners differ meaningfully from average screeners in both risk and responsiveness to information.

Our main finding is that screening information complements, rather than substitutes for, prevention. A favorable screening result lowers perceived current cancer risk, but it also raises the value of preserving future health. Empirically, this health-capital preservation channel dominates moral hazard effects, so that negative screens reduce smoking in both the experimental data and the estimated model. Counterfactual simulations show that screening policy has consequences beyond earlier diagnosis. Expanding access to screening can induce cessation, increase cancer-free years, and improve longevity, with particularly large returns when screening reaches smokers early enough for cessation to meaningfully alter subsequent disease risk. These results imply that the design of screening recommendations should account not only for clinical risk and test accuracy, but also for endogenous health behavior and selection into information acquisition. More generally, preventive care policies that reveal health information may have first-order effects on behavior, and those effects should be incorporated into both welfare analysis and the construction of clinical guidelines.

References

Aberle, D. R., Adams, A. M., Berg, C. D., Black, W. C., Clapp, J. D., Fagerstrom, R. M., et al. (2011). Reduced lung-cancer mortality with low-dose computed tomographic screening. The New England Journal of Medicine, 365(5):395–409.

Alford-Holloway, M., Triana, A., Baker, K., Iams, W., and Mullangi, S. (2024). Ep. 17e. 02 assessing the true cost of lung cancer screening-chargemaster, payer, and cash price discrepancies for ct chest imaging. Journal of Thoracic Oncology, 19(10):S720.

Alsan, M., Garrick, O., and Graziani, G. (2019). Does diversity matter for health? experimental evidence from oakland. American Economic Review, 109(12):4071–4111.

Anderson, D. M., Hoagland, A., and Zhu, E. (2024). Medical bill shock and imperfect moral hazard. Journal of Public Economics, 236:105152.

Andre, P., Haaland, I., Roth, C., Wiederholt, M., and Wohlfart, J. (2026). Narratives about the macroeconomy. The Review of Economic Studies, page rdag014. Advance article / corrected proof.

Association, A. L. et al. (2020). Lung cancer screening: coverage in health insurance plans.

Augenblick, N., Lazarus, E., and Thaler, M. (2025). Overinference from weak signals and underinference from strong signals. The Quarterly Journal of Economics, 140(1):335–401.

Baicker, K., Mullainathan, S., and Schwartzstein, J. (2015). Behavioral hazard in health insurance. The Quarterly Journal of Economics, 130(4):1623–1667.

Bandi, P., Star, J., Ashad-Bishop, K., Kratzer, T., Smith, R., and Jemal, A. (2024). Lung cancer screening in the us, 2022. JAMA Internal Medicine, 184(8):882–891.

Barsky, R. B., Juster, F. T., Kimball, M. S., and Shapiro, M. D. (1997). Preference parameters and behavioral heterogeneity: An experimental approach in the health and retirement study. The Quarterly Journal of Economics, 112(2):537–579.

Becker, G. S. and Murphy, K. M. (1988). A theory of rational addiction. Journal of political Economy, 96(4):675–700.

Bernheim, B. D. and Rangel, A. (2004). Addiction and cue-triggered decision processes. American Economic Review, 94(5):1558–1590.

Bordalo, P., Conlon, J., Gennaioli, N., Kwon, S., and Shleifer, A. (2026). How people use statistics. The Review of Economic Studies, 93(1):250–285.

Brain, K., Carter, B., Lifford, K. J., Burke, O., Devaraj, A., Baldwin, D. R., Duffy, S., and Field, J. K. (2017). Impact of low-dose CT screening on smoking cessation among high-risk participants in the UK Lung Cancer Screening Trial. Thorax, 72(10):912–918.

Burus, T., McAfee, C. R., Knight, J. R., Mullett, T. W., and Hull, P. C. (2026). Lung cancer screening prevalence and changes in 2024. JAMA Internal Medicine, 186(6). Published online April 27, 2026.

Campaign for Tobacco-Free Kids (2026). Campaign for tobacco-free kids. https://www.tobaccofreekids.org/. Accessed: July 16, 2026.

Capatina, E. and Keane, M. P. (2026). Health shocks, health insurance, human capital, and the dynamics of earnings and health. Journal of Political Economy.

Catherine, S. and Ebrahimian, M. (2024). Robustness checks in structural analysis. Working Paper 30443, National Bureau of Economic Research.

Centers for Medicare & Medicaid Services (2015). Screening for lung cancer with low dose computed tomography (ldct) (cag-00439n): Decision memo. National Coverage Analysis; accessed 2026-05-11.

Centers for Medicare & Medicaid Services (2022). National Coverage Determination (NCD): Lung Cancer Screening with Low Dose Computed Tomography (LDCT) (210.14). https://www.cms.gov/medicare-coverage-database/view/ncd.aspx?NCDId=364. Version 2; effective February 10, 2022. Accessed May 11, 2026.

Chan, T. Y. and Hamilton, B. H. (2006). Learning, private information, and the economic evaluation of randomized experiments. Journal of Political Economy, 114(6):997–1040.

Chandra, A., Gruber, J., and McKnight, R. (2010). Patient cost-sharing and hospitalization offsets in the elderly. American Economic Review, 100(1):193–213.

Ching, A. T., Erdem, T., and Keane, M. P. (2013). Invited paper—learning models: An assessment of progress, challenges, and new developments. Marketing Science, 32(6):913–938.

Crawford, G. S. and Shum, M. (2005). Uncertainty and learning in pharmaceutical demand. Econometrica, 73(4):1137–1173.

Darden, M. (2017). Smoking, expectations, and health: A dynamic stochastic model of lifetime smoking behavior. Journal of Political Economy, 125(5):1465–1522.

Darden, M., Gilleskie, D. B., and Strumpf, K. (2018). Smoking and mortality: New evidence from a long panel. International economic review, 59(3):1571–1619.

Darden, M. E. and Hoagland, A. (2025). Lung cancer screening and uspstf recommendations. JAMA Network Open, 8(2):e2458916–e2458916.

de Koning, H. J., van der Aalst, C. M., de Jong, P. A., et al. (2020). Reduced lung-cancer mortality with volume CT screening in a randomized trial. The New England Journal of Medicine, 382(6):503–513.

de Paula, Á., Shapira, G., and Todd, P. E. (2014). How beliefs about HIV status affect risky behaviors: Evidence from Malawi. Journal of Applied Econometrics, 29(6):944–964.

DeCicca, P., Kenkel, D., and Lovenheim, M. F. (2022). The economics of tobacco regulation: A comprehensive review. Journal of Economic Literature, 60(3):883–970.

Delavande, A. and Kohler, H.-P. (2016). HIV/AIDS-related expectations and risky sexual behaviour in Malawi. The Review of Economic Studies, 83(1):118–164.

Doll, R., Peto, R., Boreham, J., Gray, R., and Sutherland, I. (2004). Mortality in Relation to Smoking: 50 Years' Observations on Male British Doctors. British Medical Journal, 328:1519–1528.

Duarte, G. and Fonseca, J. (2023). Global identification with gradient-based structural estimation. Working paper.

Ehrlich, I. and Becker, G. S. (1972). Market insurance, self-insurance, and self-protection. Journal of Political Economy, 80(4):623–648.

Einav, L., Finkelstein, A., Oostrom, T., Ostriker, A., and Williams, H. (2020). Screening and Selection: The Case of Mammograms. American Economic Review, 110(12):3836–3870.

Elías, J. J., Lacetera, N., and Macis, M. (2019). Paying for kidneys? a randomized survey and choice experiment. American Economic Review, 109(8):2855–88.

Exley, C. L., Hauser, O. P., Moore, M., and Pezzuto, J.-H. (2025). Believed gender differences in social preferences. The Quarterly Journal of Economics, 140(1):403–458.

Falk, A., Becker, A., Dohmen, T., Enke, B., Huffman, D., and Sunde, U. (2018). Global evidence on economic preferences. The Quarterly Journal of Economics, 133(4):1645–1692.

Ferrario, B. and Stantcheva, S. (2022). Eliciting people's first-order concerns: Text analysis of open-ended survey questions. In AEA Papers and Proceedings, volume 112, pages 163–169. American Economic Association 2014 Broadway, Suite 305, Nashville, TN 37203.

Gilleskie, D. B. (1998). A dynamic stochastic model of medical care use and work absence. Econometrica, 66(1):1–45.

Gong, E. (2015). HIV testing and risky sexual behaviour. The Economic Journal, 125(582):32–60.

Graeber, T., Roth, C., and Zimmermann, F. (2024). Stories, statistics, and memory. The Quarterly Journal of Economics, 139(4):2181–2225.

Grossman, M. (1972). On the Concept of Health Capital and the Demand for Health. Journal of Political Economy, 80(2):223–255.

Gruber, J. and Kőszegi, B. (2001). Is addiction "rational"? theory and evidence. The Quarterly Journal of Economics, 116(4):1261–1303.

Gul, F. and Pesendorfer, W. (2007). Harmful addiction. The Review of Economic Studies, 74(1):147–172.

Haaland, I., Roth, C., Stantcheva, S., and Wohlfart, J. (2025). Understanding economic behavior using open-ended survey data. Journal of Economic Literature, 63(4):1244–1280.

Haaland, I. K., Roth, C., Stantcheva, S., and Wohlfart, J. (2024). Measuring what is top of mind. Working Paper 32421, National Bureau of Economic Research.

Henderson, L. M., Su, I.-H., Rivera, M. P., Pak, J., Chen, X., Reuland, D. S., and Lund, J. L. (2024). Prevalence of lung cancer screening in the US, 2022. JAMA Network Open, 7(3):e243190–e243190.

Hendren, N. and Sprung-Keyser, B. (2020). A unified welfare analysis of government policies. The Quarterly journal of economics, 135(3):1209–1318.

Hoagland, A. (2026). An ounce of prevention or a pound of cure? The value of health risk information. Review of Economics and Statistics.

Internal Revenue Service, Employee Benefits Security Administration, Department of Labor, and Office of Consumer Information and Insurance Oversight, Department of Health and Human Services (2010). Interim Final Rules for Group Health Plans and Health Insurance Issuers Relating to Coverage of Preventive Services Under the Patient Protection and Affordable Care Act. Federal Register, 75(137), 41726–41760. Document No. 2010-17242; TD 9493; OCIIO-9992-IFC; interim final rules with request for comments; effective September 17, 2010.

Li, Y., Li, F., Wang, G., Zeng, Q., and Xie, P. (2025). Additive impact of chronic obstructive pulmonary disease (copd) and cardiovascular disease (cvd) on all-cause and disease-specific mortality: a longitudinal nationwide population-based study. BMC Pulmonary Medicine, 25(1):275.

McGranaghan, C., Nielsen, K., O'Donoghue, T., Somerville, J., and Sprenger, C. D. (2024). Distinguishing common ratio preferences from common ratio effects using paired valuation tasks. American Economic Review, 114(2):307–347.

Miguel, E. and Kremer, M. (2004). Worms: Identifying impacts on education and health in the presence of treatment externalities. Econometrica, 72(1):159–217.

Murphy, K. M. and Topel, R. H. (2006). The value of health and longevity. Journal of political Economy, 114(5):871–904.

National Cancer Institute (2026). Colorectal cancer risk assessment calculator. https://ccrisktool.cancer.gov/calculator.html. Accessed: July 16, 2026.

Newhouse, J. P. (2021). An ounce of prevention. Journal of Economic Perspectives, 35(2):101–118.

Oster, E. (2012). HIV and sexual behavior change: Why not Africa? Journal of Health Economics, 31(1):35–49.

Pinsky, P. F., Church, T. R., Izmirlian, G., and Kramer, B. S. (2013). The National Lung Screening Trial: results stratified by demographics, smoking history, and lung cancer histology. Cancer, 119(22):3976–3983.

Pinsky, P. F., Gierada, D. S., Black, W., Munden, R., Nath, H., Aberle, D., and Kazerooni, E. (2015). Performance of Lung-RADS in the National Lung Screening Trial: a retrospective assessment. Annals of Internal Medicine, 162(7):485–491.

Polanco, D., Pinilla, L., Gracia-Lavedan, E., Mas, A., Bertran, S., Fierro, G., Seminario, A., Gómez, S., and Barbé, F. (2021). Prognostic value of symptoms at lung cancer diagnosis: a three-year observational study. Journal of thoracic disease, 13(3):1485.

Rose, L., Rajasekar, G., Nambiar, A., Pohl, A., Ruddy, K. J., Arnow, K., Patel, M., and Morris, A. M. (2025). Estimated out-of-pocket costs for patients with common cancers and private insurance. JAMA Network Open, 8(7):e2521575.

The National Lung Screening Trial Research Team (2011). Reduced lung-cancer mortality with low-dose computed tomographic screening. New England Journal of Medicine, 365(5):395–409.

Thornton, R. L. (2008). The demand for, and impact of, learning HIV status. American Economic Review, 98(5):1829–1863.

U.S. Environmental Protection Agency (2026). Mortality risk valuation. https://www.epa.gov/environmental-economics/mortality-risk-valuation. Last updated January 26, 2026. Accessed September 9, 2026.

U.S. Preventive Services Task Force (2004). Lung cancer screening: recommendation statement. Annals of Internal Medicine, 140(9):738–739.

U.S. Preventive Services Task Force (2014). Screening for lung cancer: U.s. preventive services task force recommendation statement. Annals of Internal Medicine, 160(5):330–338. PMID: 24378917.

U.S. Preventive Services Task Force (2021). Screening for lung cancer: Us preventive services task force recommendation statement. JAMA, 325(10):962–970.

Volk, R. J., Lowenstein, L. M., Leal, V. B., Escoto, K. H., Cantor, S. B., Munden, R. F., Rabius, V. A., Bailey, L., Cinciripini, P. M., Lin, H., Housten, A. J., Luckett, P. G., Esparza, A., Godoy, M. C., and Bevers, T. B. (2020). Effect of a patient decision aid on lung cancer screening decision-making by persons who smoke: A randomized clinical trial. JAMA Network Open, 3(1):e1920362–e1920362.

Volk, R. J., Maki, K. G., Rogova, A., Tu, A., Nguyen, C. V., Ma, H., and Hoffman, R. M. (2026). The counseling and shared decision-making visit for lung cancer screening: A thematic analysis of public comments to the centers for medicare & medicaid services during the 2021-2022 national coverage analysis process. CHEST, 169(5):1402–1414.

Wing, C., Freedman, S. M., and Hollingsworth, A. (2024). Stacked difference-in-differences. NBER Working paper.

Yoshida, K., Gowers, K. H., Lee-Six, H., Chandrasekharan, D. P., Coorens, T., Maughan, E. F., Beal, K., Menzies, A., Millar, F. R., Anderson, E., et al. (2020). Tobacco smoking and somatic mutations in human bronchial epithelium. Nature, 578(7794):266–272.

Zila, J. and Kukacka, J. (2023). Moment set selection for the simulated method of moments using simple machine learning. Journal of Economic Behavior & Organization, 211:1–20.

9 Tables

Table 1: Baseline Covariate Balance

	N	Mean	p_1	p_2	p_3
Age in Years	3912	52.298	0.567	0.769	0.526
Female	3912	0.622	0.565	0.466	0.296
Race					
White	3912	0.825	0.681	0.955	0.336
Black	3912	0.073	0.401	0.705	0.475
Other	3912	0.103	0.924	0.596	0.553
Least Risk Averse, $\gamma \in [0, 0.3]$	3880	0.053	0.733	0.576	0.354
Most Risk Averse, $\gamma \geq 7.52$	3880	0.290	0.643	0.671	0.023
Least Patient, $\beta < 0.476$	3873	0.377	0.524	0.783	0.420
Most Patient, $\beta \in [0.943, 1]$	3873	0.041	0.914	0.402	0.770
Uninsured	3912	0.080	0.957	0.733	0.269
Income					
Less than $25,000	3908	0.161	0.632	0.712	0.194
$25,000-$49,999	3908	0.241	0.557	0.549	0.176
$50,000-$99,999	3908	0.349	0.294	0.922	0.831
$100,000-$199,999	3908	0.209	0.895	0.827	0.555
More than $200,000	3908	0.040	0.768	0.578	0.222
Currently Smoke Cigarettes.	3912	0.343	0.226	0.785	0.725
Pack-Years	3912	27.779	0.840	0.396	0.754
Eligibility for Free Screening	3912	0.242	0.714	.	0.593
Age Eligible	3912	0.527	0.339	0.844	0.173
Pack-Years Eligible	3912	0.530	0.822	0.070	0.601
Smoking Eligible	3912	0.710	0.382	0.946	0.451
Belief of Early-Stage Lung Cancer	3851	22.170	0.232	0.981	0.144
Lower Expected Risk	3912	0.234	0.733	0.216	0.966
About the Same.	3912	0.533	0.357	0.070	0.671
Higher Expected Risk	3912	0.233	0.040	0.591	0.647
Belief of True Positive	3851	64.370	0.755	0.466	0.866
Belief of False Positive	3827	17.901	0.850	0.990	0.859
High Stigma	3909	0.453	0.028	0.531	0.036
Avoids Information	3912	0.171	0.768	0.162	0.840

Notes: Table 1 presents the overall mean of key variables and three p-values. The first p-value is of the F-test that there are no differences in means between the control arm and the three treatment arms quality, stigma, and price. The second p-value is on the F-test of no differences in means between the lowest price treatment ($100) and the other two prices ($300 and $500) conditional on being randomized to the price arm and being ineligible for free screening. The final p-value is on the t-test that there is no difference in means between the treatment and control arm of the smoking experiment.

Table 2: Moments Used in Estimation

	Moment	Individual contribution g_i (estimation sets $\frac{1}{N}\sum_i g_i = 0$)	Source
Smoking behavior			
1	Smoking rates by age	$g_i = s_i - s^*_{k(a_i)}$	BRFSS
2	Smoking reinforcement residuals (slopes and intercept)	$r_i \equiv 100\, s_i - (17.126 + 1.105\, h_i - 0.009\, h_i^2)$	BRFSS
Screening levels and gradients (alive, $\theta_i < 3$)			
3	Screening by USPSTF eligibility	$g_i = \begin{cases} x_i - 0.2537 & \text{ineligible} \\ x_i - 0.5163 & \text{eligible} \end{cases}$	Survey
4	Screening by age, high pack-year	$g_i = x_i - \bar{x}^{*,H}_{k(a_i)}$	(Darden and Hoagland, 2025)
5	Screening by age, low pack-year	$g_i = x_i - \bar{x}^{*,L}_{k(a_i)}$	(Darden and Hoagland, 2025)
6	Screening by history, young	$g_i = x_i - \bar{x}^{*,Y}_{m(h_i)}$	(Darden and Hoagland, 2025)
7	Screening by history, old	$g_i = x_i - \bar{x}^{*,O}_{m(h_i)}$	(Darden and Hoagland, 2025)
Experimental treatment effects (alive, $\theta_i < 3$; $w_k = N/N_k$)			
8	Stigma effect (type 1 − type 2)	$g_i = w_1(x_i - 0.08)\mathbf{1}[\nu_i{=}1] - w_2\, x_i\, \mathbf{1}[\nu_i{=}2]$	Survey
9	Stigma effect (type 3 − type 4)	$g_i = w_3(x_i - 0.08)\mathbf{1}[\nu_i{=}3] - w_4\, x_i\, \mathbf{1}[\nu_i{=}4]$	Survey
10	Optimism effect (type 3 − type 1)	$g_i = w_3(x_i - 0.21)\mathbf{1}[\nu_i{=}3] - w_1\, x_i\, \mathbf{1}[\nu_i{=}1]$	Survey
11	Optimism effect (type 4 − type 2)	$g_i = w_4(x_i - 0.21)\mathbf{1}[\nu_i{=}4] - w_2\, x_i\, \mathbf{1}[\nu_i{=}2]$	Survey
12	Price elasticity for screening	$g_i = (x_i - \bar{x}_i^-) - 0.17\, \bar{x}_i^-$, when i becomes USPSTF eligible.	Survey
Disease and beliefs			
13	Cancer incidence by age	$g_i = \mathbf{1}[\theta_i \geq 2] - \pi^*_{k(a_i)}$	SEER
14	Average beliefs	$\begin{cases} g_i = b_i - 0.2217 & \text{no cancer} \\ 0 & \text{else} \end{cases}$	Survey

Notes: Table lists all moments used in estimating the model, following Section 6. For each moment, we list the individual moment conditions and target values as well as the source of moments to match. See Table 4 for discussion of which moments correspond to which model parameters. In estimation, each moment is calculated as an individual (person-period) contribution g_i; simulated GMM chooses parameters so that the sample mean of each column is zero, matching simulated moments to the data targets. Age bins $k(\cdot)$ and pack-year bins $m(\cdot)$ are 5-year: $a \in \{<45, 45\text{–}50, \ldots, 75\text{–}80, \geq 80\}$ and $h \in \{<5, 5\text{–}10, \ldots, 35\text{–}40, \geq 40\}$. Screening scalar targets are the baseline intent-to-screen mean of 0.3825 less the price effect 0.1288 (ineligible, = 0.2537) and 0.5163 for USPSTF-eligible individuals; the stigma and optimism effects (0.08 and 0.21) and the 17% price response (0.17) come from the experimental (Prolific) data; the average-belief target is 0.2217. All other bin targets are available in replication code.

Table 3: Calibrated Model Parameters

	Notation	Calibrated Value	Bounds	Source
Preferences & Time				
Discount factor	β	0.95	[0.90, 0.99]	Survey
CRRA risk-aversion coefficient	γ_0	2	[1.01, 5]	Survey
Terminal age	T	100	[90, 110]	—
Prices & Income (annual, USD)				
Price of smoking	p_s	\$3,285	[\$2,920, \$3,650]	(Campaign for Tobacco-Free Kids, 2026)
Price of LDCT screening (if OOP)	p_x	\$300	[\$100, \$500]	(Alford-Holloway et al., 2024)
Annual cancer treatment cost (OOP)	p_y	\$5,000	[\$3,000, \$10,000]	(Rose et al., 2025)
Annual income	W	\$63,500	[\$50,000, \$80,000]	Survey
Screening Test Quality				
True positive rate	ρ	0.703	[0.60, 0.85]	Truveta
Subjective true positive rate	$\hat{\rho}$	0.644	[0.50, 0.80]	Survey
False positive rate	λ	0.121	[0.05, 0.20]	Truveta
Subjective false positive rate	$\hat{\lambda}$	0.179	[0.10, 0.25]	Survey
Symptom Probabilities				
Pr(symptom $\mid \theta = 1$)	$\Pr(\eta \mid \theta = 1)$	0.033	[0.02, 0.10]	(Polanco et al., 2021)
Pr(symptom $\mid \theta = 2$)	$\Pr(\eta \mid \theta = 2)$	0.064	[0.03, 0.20]	(Polanco et al., 2021)
Pr(symptom $\mid \theta = 3$)	$\Pr(\eta \mid \theta = 3)$	0.246	[0.15, 0.50]	(Polanco et al., 2021)
Early Lung Cancer				
Intercept	α_0	-6.739	[-7.5, -5]	NLST (see Appendix Table 3)
Smoking history (per 10 pack-years)	α_1	0.1245	[0.05, 0.20]	NLST
Currently smoking	α_2	0.977	[0.75, 1.25]	NLST
Age (per decade above 40)	α_3	1.70	[1.30, 2.10]	NLST
Age^2 (per decade above 40)^2	α_4	-0.16	[-0.2, 0]	NLST
Lung-Cancer Progression				
Intercept	ζ_0	-2.713	[-4, -1]	NLST (see Appendix Table 3)
Years since early-stage onset	ζ_1	0.309	[0.1, 0.5]	NLST
Treatment	ζ_2	-0.210	[0, -0.4]	NLST
Treatment × years since onset	ζ_3	-0.286	[-0.6, -0.05]	NLST
Currently smoking	ζ_4	0.390	[0.2, 0.6]	NLST
Chronic-Condition Onset				
Intercept	ψ_0	-4.14	[-5, -3]	(National Cancer Institute, 2026)
Currently smoking	ψ_1	1.30	[0.7, 2]	(National Cancer Institute, 2026)
Age (per decade above 40)	ψ_2	0.81	[0.4, 1.2]	(National Cancer Institute, 2026)
Smoking × Age	ψ_3	-0.34	[-0.7, 0]	(National Cancer Institute, 2026)
Mortality				
Intercept	ω_0	-5.40	[-6.5, -4.5]	(Li et al., 2025)
Early-stage cancer indicator	ω_1	1.37	[0.80, 2]	(Li et al., 2025)
Late-stage cancer indicator	ω_2	3.57	[2.5, 4.5]	(Li et al., 2025)
Other chronic condition	ω_3	0.58	[0.30, 1]	(Li et al., 2025)
Age (per decade above 40)	ω_4	0.77	[0.5, 1.1]	(Li et al., 2025)

Notes: Table lists all parameters defined in Section 4 that were calibrated externally rather than estimated via GMM. (Estimated parameters are discussed in Table 4.) For each calibrated parameter, we indicate the calibrated value of each parameter, reasonable bounds used in assessing model robustness, and the relevant source for the calibration. Chronic condition onset parameters were constructed based on pooled health risk tables. Mortality transition parameters used the reference above in conjunction with life expectancy tables and SEER data. For each logistic regression, intercepts were calibrated to match baseline averages in BRFSS and Prolific Survey data to make populations comparable.

Table 4: Estimated Model Parameters

Parameter	Notation	Estimated Value	95% CI	Identifying Moment
Health-State Utility				
Utility level, no/early cancer	$U_{\theta<3}$	8.5×10^6	$[8.45, 8.55] \times 10^6$	Screening and cancer rates
Utility level, late-stage cancer	$U_{\theta=3}$	9.8×10^7	$[9.79, 9.81] \times 10^7$	Screening and cancer rates
Smoking Preferences				
Smoking utility (flow)	γ_1	-3.6×10^5	$[-3.64, -3.57] \times 10^5$	Smoking prevalence
Smoking × history (linear)	γ_2	7.3×10^4	$[7.29, 7.32] \times 10^4$	Smoking/history relationship
Smoking × history^2 (quadratic)	γ_3	993	$[990, 996]$	Smoking/history relationship
Screening Disutility & Costs				
Screening disutility, baseline	$\gamma_{4,0}$	-6.5×10^5	$[-6.51, -6.49] \times 10^5$	Screening, beliefs
Stigma effect $\nu = 2$	$\gamma_{4,1}$	-8.0×10^5	$[-8.01, -7.99] \times 10^5$	Experiment
Pessimism effect $\nu = 3$	$\gamma_{4,2}$	-9.4×10^6	$[-9.47, -9.33] \times 10^6$	Experiment
Interaction $\nu = 4$	$\gamma_{4,3}$	-8.6×10^5	$[-8.61, -8.59] \times 10^5$	Experiment
Disutility, $s of OOP spending	γ_5	−6,639	[−6,659, −6,619]	Experiment
Disutility, symptoms	γ_6	-5.2×10^5	$[-5.20, -5.20] \times 10^5$	Beliefs, cancer rates
Cancer Beliefs, Age 40				
Average	b_0	0.112	$[0.1115, 0.1125]$	Subjective beliefs
SD	—	0.18	—	Subjective beliefs
IQR	—	[0.030, 0.120]	—	—

Notes: Table lists all parameters defined in Section 4 that were estimated via GMM. (Calibrated parameters are discussed in Table 3.) For each estimated parameter, we list the value from the preferred specification, the 95% confidence interval, and the relevant moment used in identification (see Table 2 for a list of all moments used in estimation).

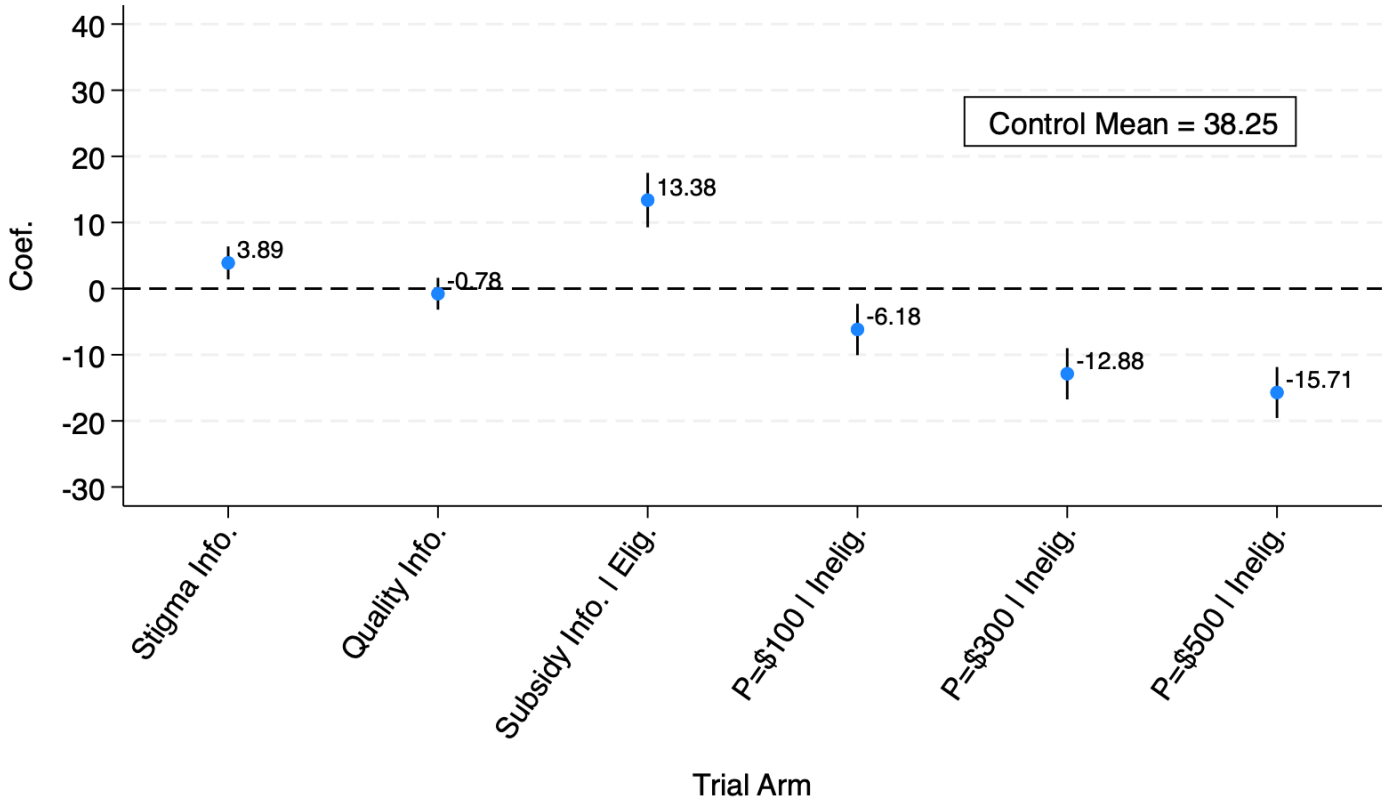
Table 5: Counterfactual Simulation Results

		% Experiencing Increase In					
Counterfactual	(1) Screening	(2) Quitting Years	(3) Cancer-Free Years	(4) YOL Gained	(5) Utility Gained	(6) % Benefiting	(7) Per-Person Value ($)
Panel A: Screening Prices							
Free Screening	213%	34.5%	5.9%	4.9%	4.9%	100%	[527,730, 600,740]
Panel B: USPSTF Eligibility Requirements							
Age: 50 to 45	12.0%	2.5%	0.01%	0.01%	0.35%	40.9%	[37,695, 42,910]
History: 20 to 10	60.7%	12.1%	2.0%	1.5%	0.56%	73.1%	[60,312, 68,656]
Panel C: Targeting Based on Preferences							
No Pessimism	81.7%	30.7%	5.0%	4.4%	5.99%	44.0%	[645,123, 734,374]
No Stigma	22.9%	6.8%	0.8%	0.6%	0.47%	47.4%	[50,619, 57,622]
Eliminating Both	124%	35.6%	5.9%	5.2%	7.09%	70.5%	[763,593, 869,234]

Notes: Table shows behavioral responses to counterfactual policies surrounding lung cancer screening. Screening results are measured near the changes in screening eligibility (between ages 40 and 60); all other results are for outcomes between ages 40 and the simulated end of life (max age = 100). Column (1) indicates percentage changes in the average screening rate at the individual-year level. Columns (2) through (4) estimate the percentage of individuals with increases in years without smoking, years without (any) cancer, and years of life, respectively. Finally, column (5) reports percentage differences in discounted lifetime utility calculated at age 40, and column (6) indicates the percentage of the sample with a positive net utility change as a result of the policy. In column (7), we scale these in dollars based on a range of estimates for the value of remaining life at age 40 from prior literature, as discussed in the text. Baseline simulations are computed with simulated dataset of 1,000,000 respondents.

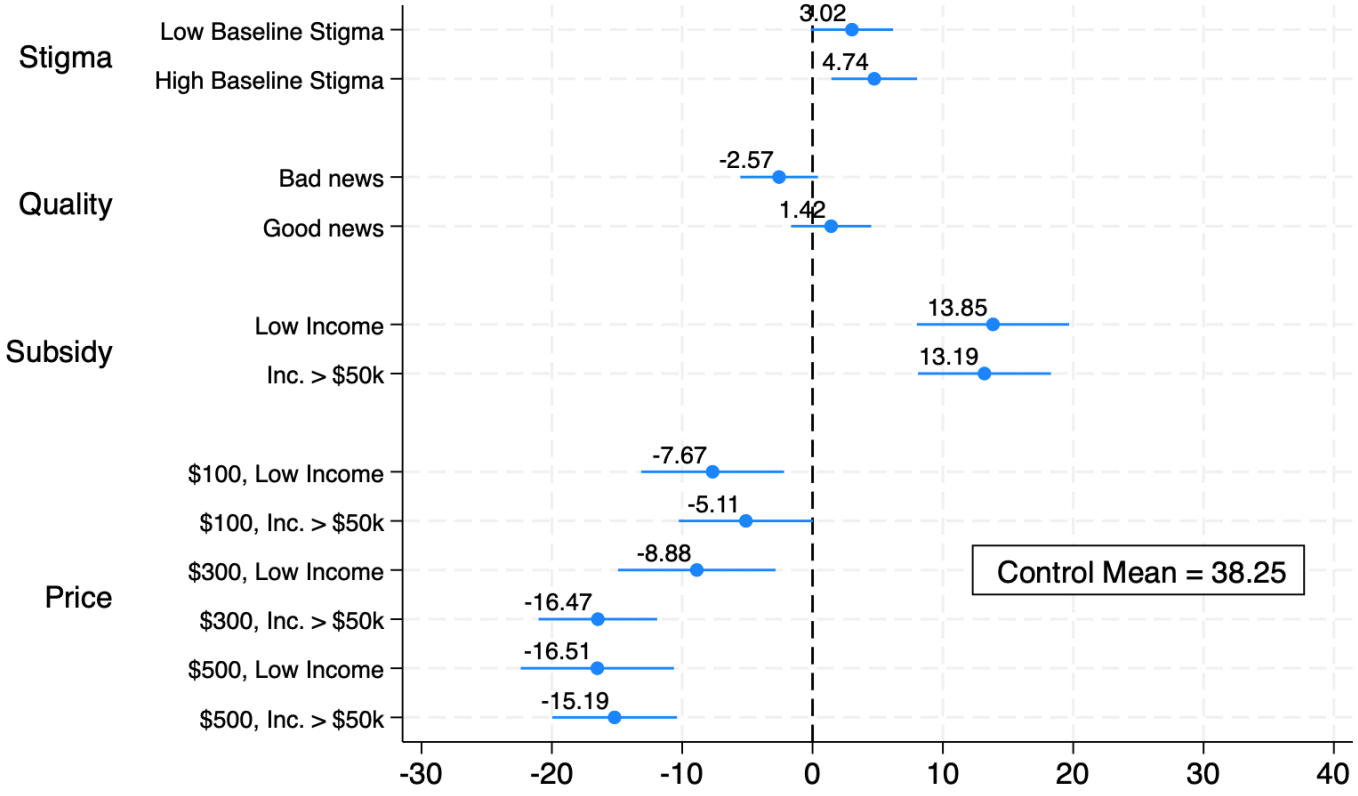
10 Figures

Figure 3: Experimental Effects on Intent to Screen



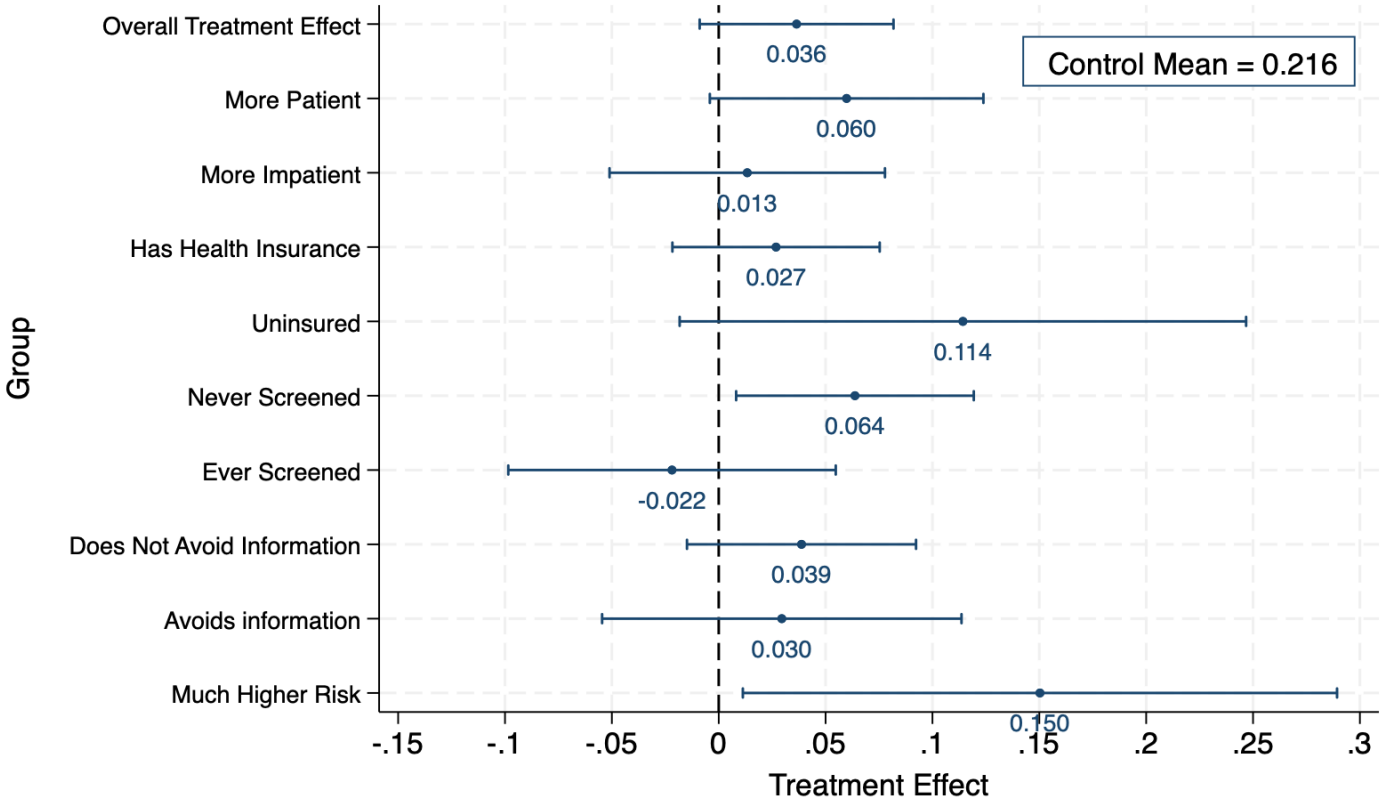
Notes: The Figure presents experimental effects from regressions of the intention to screen in the next year on binary variables for each treatment arm relative to the baseline, neutral framing of the intention to screen question. Treatment arms include receiving information about nonjudgmental screening staff (stigma), the observed false positive rate (quality info) and prices. If randomized to the price arm, eligible respondents received information about their eligibility; ineligible respondents received a price quote between $100 and $500. Coefficients are conditional on baseline characteristics in Table 1. Confidence intervals reflect robust standard errors. $n = 3,912$.

Figure 4: Heterogeneous Effects on Intent to Screen



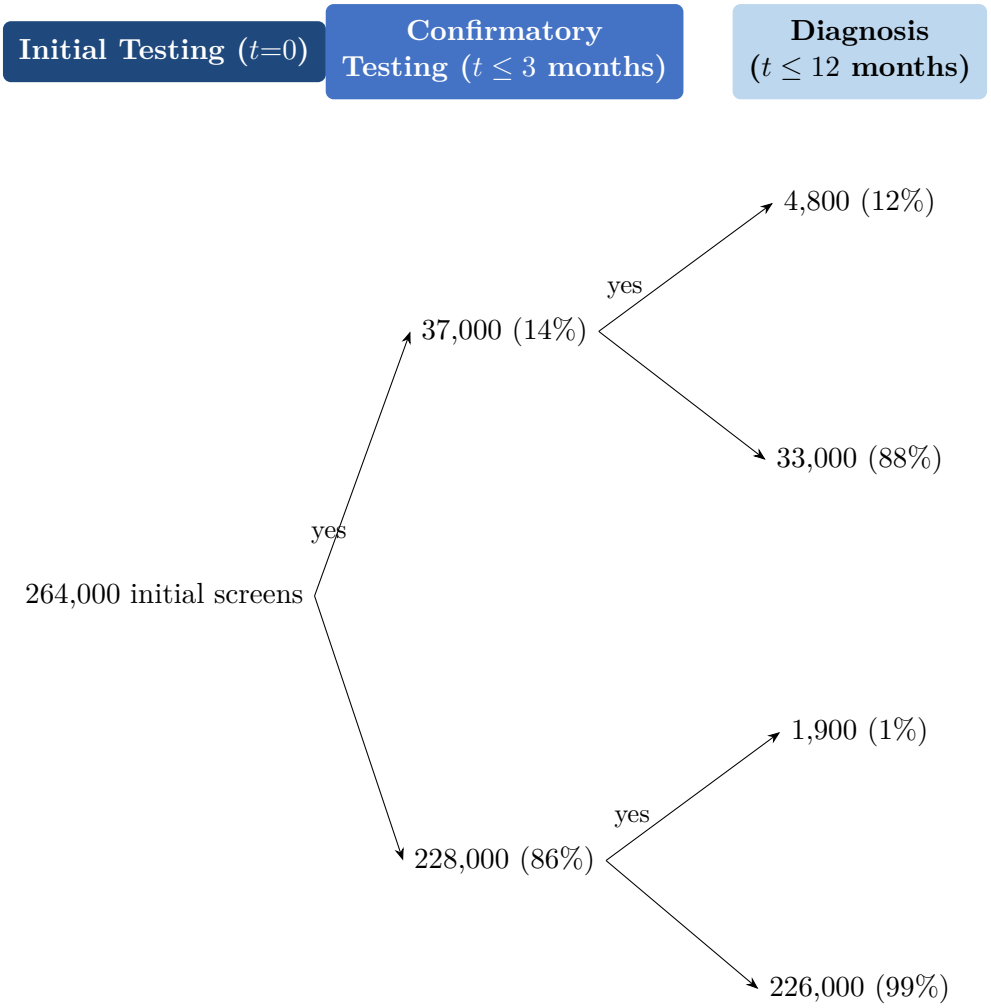
Notes: The Figure presents experimental effects from regressions of the intention to screen in the next year on binary variables for each treatment arm relative to the baseline, neutral framing of the intention to screen question. Each treatment arm indicator is interacted with relevant, baseline heterogeneity. High stigma indicates agreement with at least one of the stigma questions. Good news implies that the quality information treatment presented a lower false positive rate relative to baseline expectations. Price/subsidy effects are allowed to vary by whether baseline household income was less than $50k. Coefficients are conditional on baseline characteristics in Table 1. Confidence intervals reflect robust standard errors. $n = 3,912$.

Figure 5: Intention to Quit Among Smokers



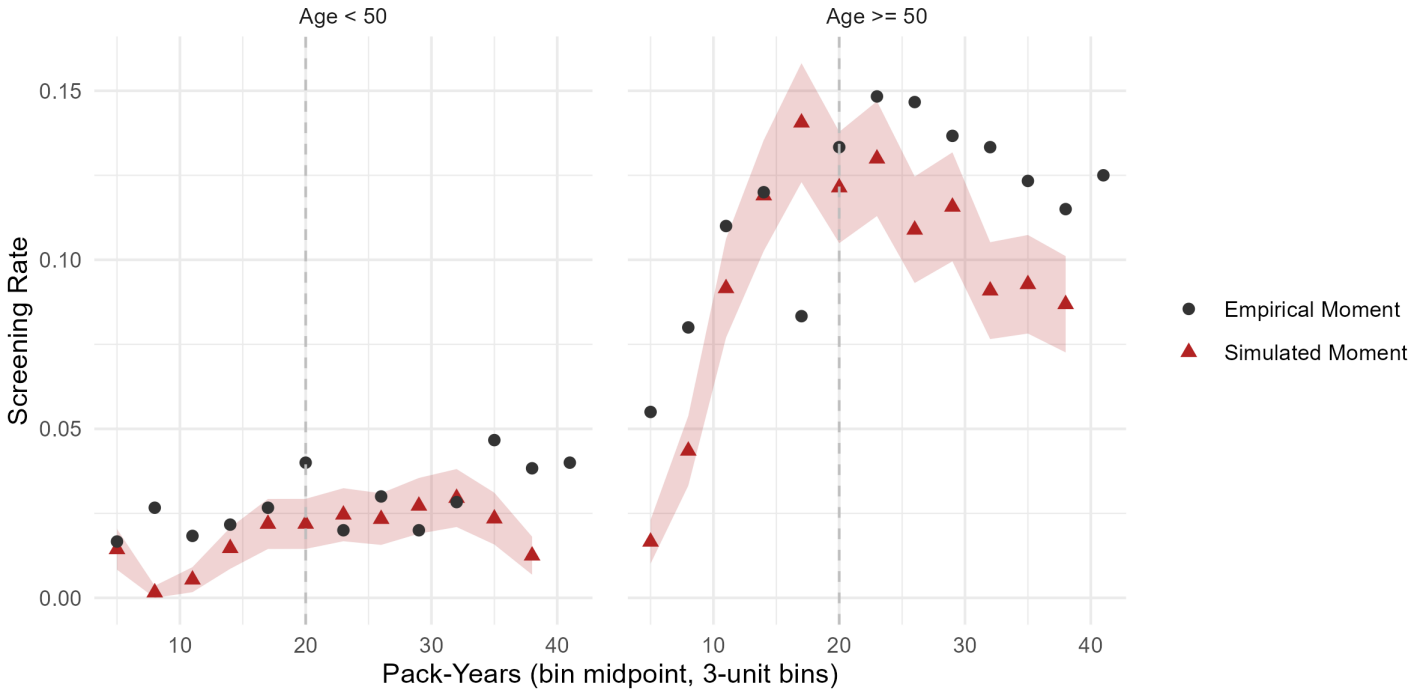
Notes: The Figure presents experimental effects on intention to quit smoking among smokers. Coefficients are treatment effects of the "clean scan" treatment group relative to the control. Coefficients are conditional on baseline characteristics in Table 1. Confidence intervals reflect robust standard errors. $n = 1,342$.

Figure 6: LDCT Screening in Truveta



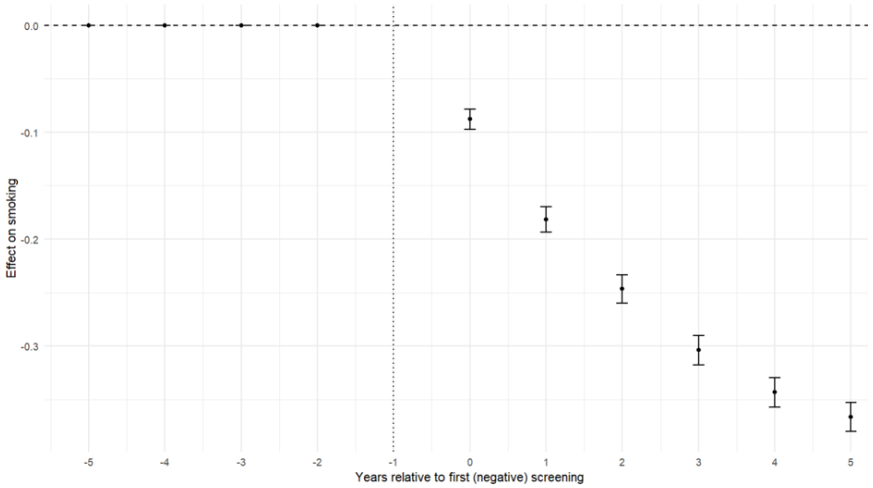
Notes: The Figure presents data from our analysis of Truveta EHR data.

Figure 7: Model Fit: Screening by Age & Smoking History



Notes: This figure plots empirical and simulated moments tracking average lung cancer screening rates. Empirical moments come from the BRFSS study (Darden and Hoagland, 2025). Sample is stratified by age and smoking history in each panel. We report binscatters averaging over 3 year or 3 pack-year increments. Confidence intervals are based on simulated sample of 500 respondents per age-smoking-history bin.

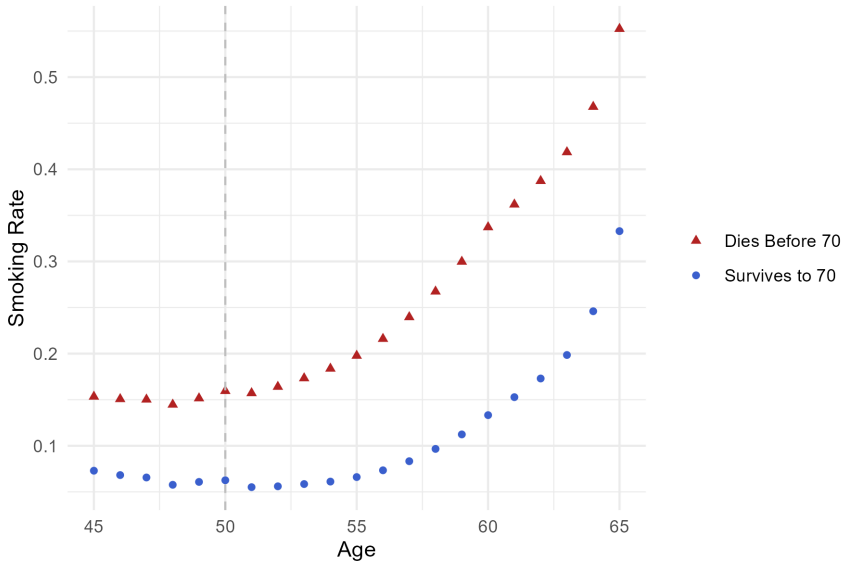
Figure 8: Model Estimate: Effect of Screening on Future Smoking Decisions



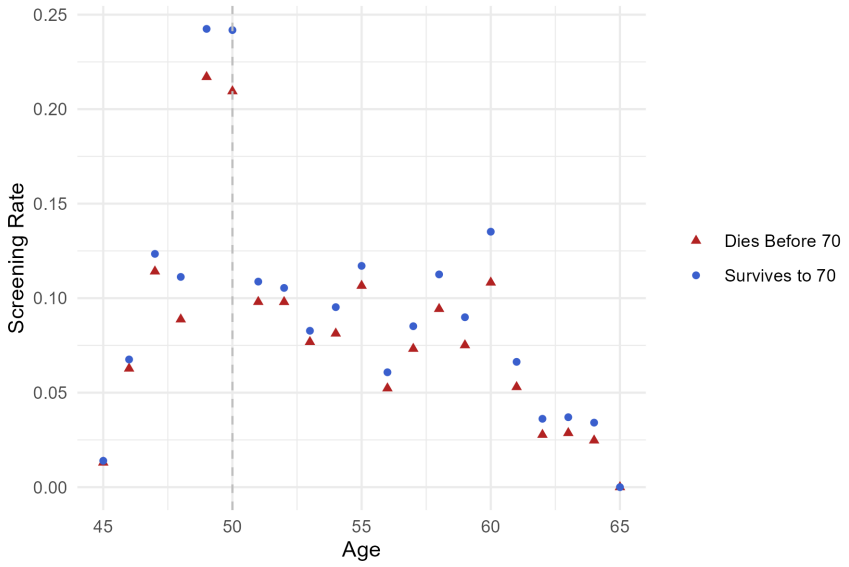
Notes: Figure plots coefficients from a stacked dynamic difference-in-differences regression estimating the effect of first screening on future smoking. Each experiment is comprised of a treatment group consisting of individuals who smoked continuously for five years prior to their first screening, and who screened for lung cancer for the first time at age $a \in [40, 70]$; the control group consists of all individuals who also smoked continuously for five years prior to the placebo screening date at age a, but who did not screen for the first time until at least $a + 5$ years later. Regression adjusts for individual, experiment, and age fixed effects (note that age and experiment fixed effects are colinear) and clusters standard errors at the individual level. Point estimates therefore represent the differences in average smoking rates in the years around screening, relative to the year prior to screening and differenced relative to the clean control group.

Figure 9: Screening & Smoking Decisions by Survival to Age 70

(a) Smoking



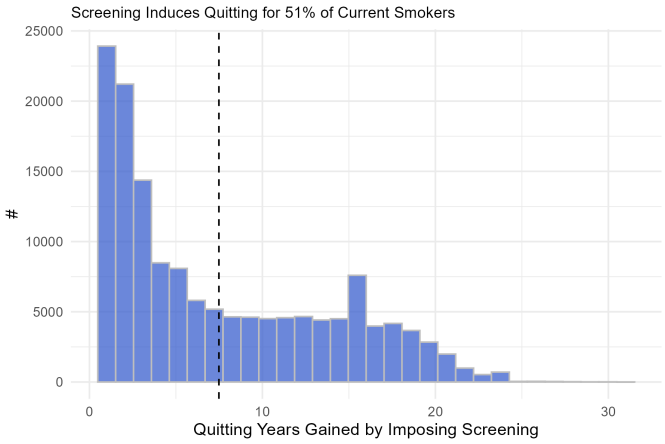
(b) Screening



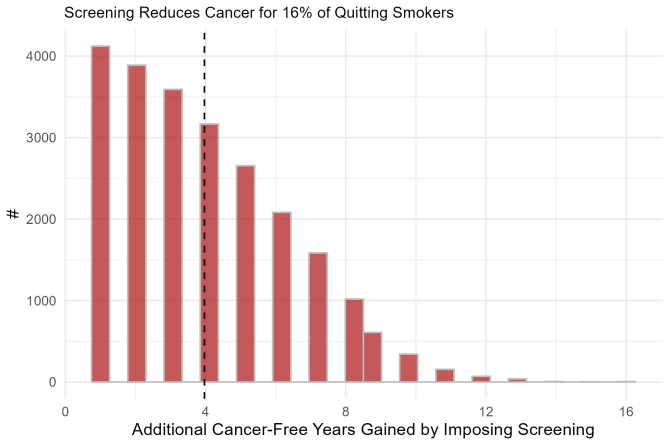
Notes: This figure plots simulated smoking and screening behaviors by age for two groups in the model: those whose simulated behaviors result in death before age 70, and those who survive to at least age 70.

Figure 10: Counterfactual Simulation: Effect of Universal Screening at Age 45

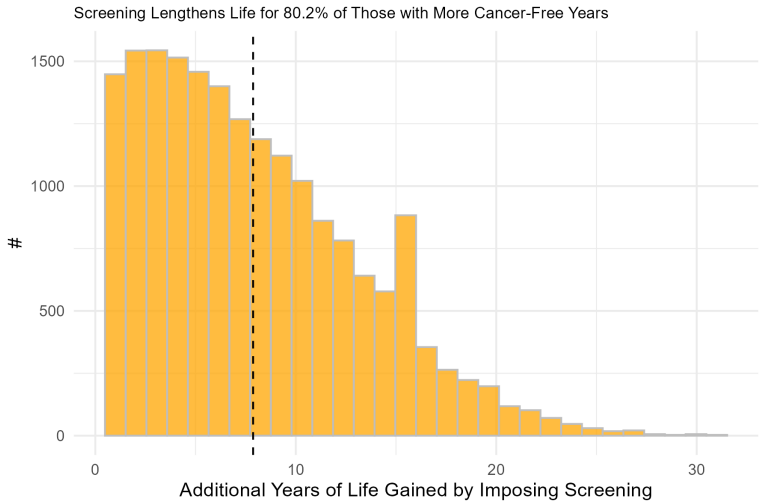
(a) Effect on Smoking Cessation



(b) Effect on Cancer Development



(c) Effect on Longevity



Notes: Figures plot results from a counterfactual simulation comparing baseline choices to a world where universal screening takes place at age 45. Each panel indicates how this simulation affects key outcomes, including smoking, cancer development, and mortality. In panel (a), the average rate and conditional amount of gained years of smoking cessation is shown for those who were current smokers before the universal screening (age 44); in panel (b), the average rate and conditional amount of gained years without cancer is shown for the same population. In panel (c), we restrict only to those who were current smokers at age 44 and those who gained additional years without cancer, and plot the average rate and conditional amount of added years of life gained from the policy.

Endogenous Screening and Health Behaviors: APPENDIX*

Michael Darden and Alex Hoagland

September 11, 2026

Abstract

Keywords:

JEL Classification:

*Darden: Johns Hopkins University Hoagland: University of Toronto

Timeline of Policy Changes



1 Structural Model

Screening Decision. The model's implications for screening can be best understood by considering the threshold of risk beliefs that trigger screenings. Screening is useful in the model as it may induce treatment, thereby increasing survival values, as well as for its value in resolving uncertainty about one's future cancer risks. Hence, if we fix other objects in the model, including prices, wealth, and individual type, then a screening decision for a given individual with a specific age, smoking history, and current smoking decision will screen if and only if:

$$x_t = 1 \iff Q^S(\tilde{b}_t) \geq Q^N(\tilde{b}_t),$$

where we let Q^S be the value from screening and Q^N be the value from not screening. Here, the relevant belief entering the decision is the symptom-updated belief, $\tilde{b}_t$.[1]

Given this, we can define the screening gain as

$$\Delta(\tilde{b}_t) \equiv Q^S(\tilde{b}_t) - Q^N(\tilde{b}_t).$$

This implicitly defines a belief threshold, $\bar{b}$, as the solution to $\Delta(\bar{b}) = 0$. Any belief above this threshold will trigger screening.

A fully-derived, closed form solution for this threshold would be unwieldy. However, we can derive important comparative statics for this threshold (and hence, screening decisions) even by considering current payoff effects separate from future informational value.

To see this, let

$$u_t^S(\tilde{b}_t) = (1 - \tilde{b}_t)\Big[(1 - \hat{\lambda})u_0^- + \hat{\lambda}u_0^+\Big] + \tilde{b}_t\Big[(1 - \rho)u_1^- + \hat{\rho}u_1^+\Big],$$

where $u_t^S(\tilde{b}_t)$ is the current period utility with screening (let u_t^N be the current period utility with no screening). Then

$$\Delta(\tilde{b}_t) = \underbrace{\left(u_t^S(\tilde{b}_t) - u_t^N\right)}_{\text{current-period net benefit}} + \beta \times \underbrace{\Big(\mathcal{C}^S(\tilde{b}_t) - \mathcal{C}^N(\tilde{b}_t)\Big)}_{\text{continuation information value}}.$$

Although closed-form solutions for the continuation values cannot easily be expressed analytically, the first term is still affected by the cost of screening, type-specific screening disutility, any utility consequences of treatment after a positive result, and any immediate utility differences from learning one's status. To see this, suppose that the only

[1] Appendix Section 3 provides definitions for Q^S and Q^N implied by the model.

benefit of screening is expected resolution or treatment benefit in the current period. Then, screening occurs when

$$(1-\tilde{b}_t)\Big[(1-\hat{\lambda})u_0^- + \hat{\lambda}u_0^+\Big] + \tilde{b}_t\Big[(1-\hat{\rho})u_1^- + \hat{\rho}u_1^+\Big] \geq u_t^N.$$

This gives the static cutoff

$$\tilde{b}_t \geq \bar{b}^{static} \equiv \frac{u_t^N - (1-\hat{\lambda})u_0^- + \hat{\lambda}u_0^+}{\Big[(1-\hat{\rho})u_1^- + \hat{\rho}u_1^+\Big] - \Big[(1-\hat{\lambda})u_0^- + \hat{\lambda}u_0^+\Big]}.$$

This cutoff, although incomplete, still highlights several important ways in which screening decisions respond to a person's type or environment. First, higher screening costs raise u_t^N relative to screening utility, thereby increasing the implicit threshold. At the same time, increased stigma (which imposes a type-specific disutility from screening) will likewise raise the threshold necessary to induce screening, while optimism about a test's outcome will reduce it. Finally, a higher perceived cancer payoff from early detection lowers the threshold and may induce additional screening.

Smoking Decision A critical insight from the model is that the decision to screen has ambiguous implications for subsequent smoking choices. A screen may generate moral hazard effects that might induce smoking, as a negative screen lowers the level of perceived cancer risk under either smoking choice. On the other hand, both positive and negative screens may improve expectations of future healthy utility, as a positive screen improves objective survival through early treatment while a negative screen gives the individual better posterior odds of being in a long-lived state. This can increase the continuation-value cost of smoking after a favorable screen, reducing the incentive to smoke or even generating cessation incentives. Both the moral hazard and the health preservation channels matter for smoking because agents are forward looking and smoking is addictive, so smoking impacts both current and future utility as well as worsening future risks and therefore the value of future life.

To see this, let $Q_j^s(\Gamma)$ represent the indirect utility from smoking for an agent, given their optimal screening decision:

$$Q_j^s(\Gamma) = \max_{x\in\{0,1\}} E\left[u(j,x;\,\Gamma) + \beta(1-P(D_{t+1}=1))V(\Gamma_{t+1}) \mid \Gamma, s=j,x\right],$$

for $j \in \{0,1\}$. The individual smokes when

$$Q_1^s(\Gamma) - Q_0^s(\Gamma) \geq 0.$$

A negative screen changes this comparison through the posterior belief state. In particular, after a negative signal,

$$\hat{b}_t^0 = \frac{(1-\hat{\rho})\tilde{b}_t}{(1-\hat{\rho})\tilde{b}_t + (1-\hat{\lambda})(1-\tilde{b}_t)},$$

which is below $\tilde{b}_t$ whenever the test is perceived to be informative, $\hat{\rho} > \hat{\lambda}$. This lower posterior may increase smoking by reducing perceived cancer risk: under either smoking choice, the next-period belief

$$B(b, s) = b + (1-b)\,\pi_{12}(h, s, a)$$

is lower when $b = \hat{b}_t^0$ than when $b = \tilde{b}_t$. This is the standard moral-hazard channel.

However, the model also generates an opposing force. The incremental effect of smoking on next-period cancer beliefs is

$$B(b,1) - B(b,0) = (1-b)\left[\pi_{12}(h,1,a) - \pi_{12}(h,0,a)\right].$$

Thus, when smoking raises cancer onset risk, a favorable screen can increase the marginal future health cost of smoking by moving the individual into a state with a larger stock of expected healthy life at risk. At the same time, this favorable information also raises the continuation value of survival, further reducing incentives to smoke. Screening may therefore complement preventive health behaviors, and might even induce quitting if the value-of-life effect dominates the moral hazard effect. The model does not sign this relationship ex ante; the direction of the smoking response is an empirical object disciplined by the smoking-intention experiment and the estimated dynamic policy functions.

Derivation of Screening Belief Threshold If the person does not screen, current utility is just the no-screen utility, and next period belief is

$$b_{t+1}^N = \tilde{b}_t + (1-\tilde{b}_t)\pi_{12}.$$

Hence,

$$Q^N(\tilde{b}_t) = u_t^N(x_t) + \beta\mathbb{E}\left[(1 - P(D_{t+1}=1))V(\Gamma_{t+1}) \mid b_{t+1} = b_{t+1}^N, x_t\right].$$

Here $u^N(x_t)$ is the per-period utility holding the smoking choice fixed.

On the other hand, if the person screens, expected utility in the current period averages over: whether there is cancer or not, weighted by $\tilde{b}_t$, and screening outcomes, weighted by subjective test beliefs (ρ, λ). We can therefore

define

$$Q^S(\tilde{b}_t) = (1-\tilde{b}_t)\Big[(1-\lambda)M_0^- + \lambda M_0^+\Big] + \tilde{b}_t\Big[(1-\rho)M_1^- + \rho M_1^+\Big],$$

where we define objects:

- M_0^-: value if true state is no cancer and the screen is negative
- M_0^+: value if true state is no cancer and the screen is positive (false positive, then confirmatory testing)
- M_1^-: value if there is cancer and the screen is negative (false negative)
- M_1^+: value if there is cancer and the screen is positive (true positive, then confirmatory testing and treatment)

Given this, we can define the screening gain as

$$\Delta(\tilde{b}_t) \equiv Q^S(\tilde{b}_t) - Q^N(\tilde{b}_t).$$

This implicitly defines a belief threshold, $\bar{b}$, as the solution to $\Delta(\bar{b}) = 0$. Any belief above this threshold will trigger screening.

2 Survey & Experimental Design

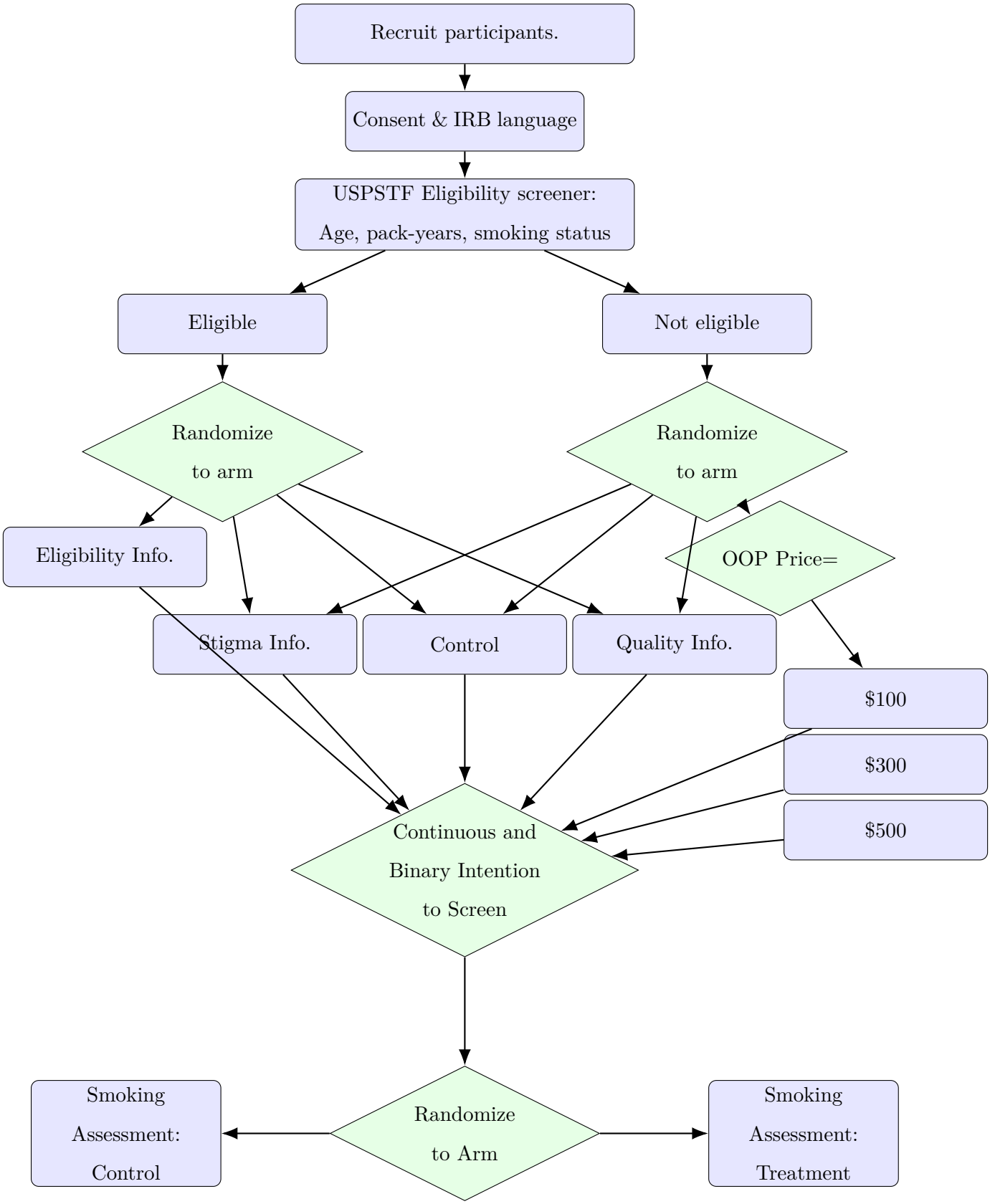


Table 1: Sample Construction

	Count
Attempted Survey	4,000
Completed Survey	3,996
ReCaptcha≥0.5	3,925
Non-missing Experimental Data	3,912

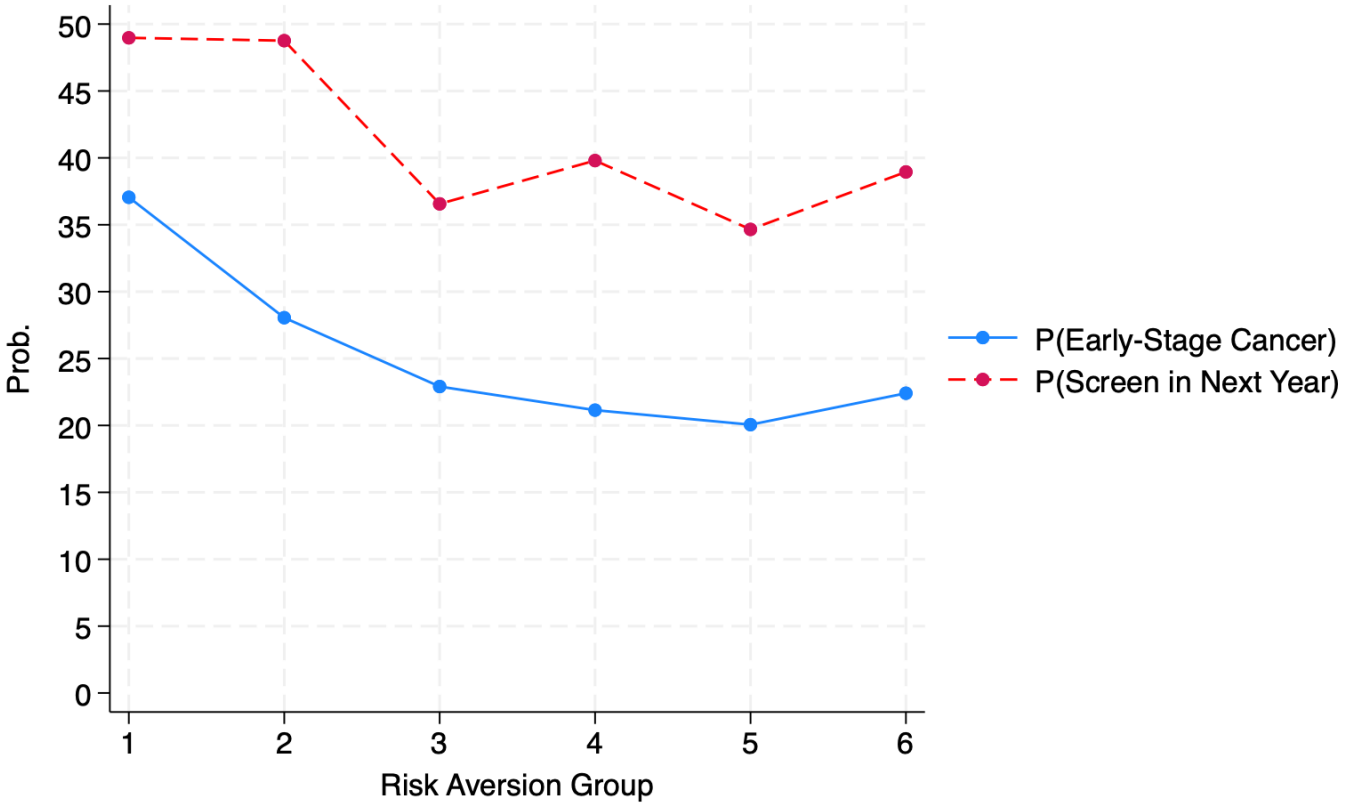
Notes: Analysis sample construction from the lung cancer screening survey. The survey was built on Qualtrics and run on Prolific from November 20th, 2025 through February 15th, 2026. The ReChaptcha score is a summary measure of whether respondent behavior is consistent with a real person. Scores less than 0.5 are associated with bot behavior. See Qualtrics fraud detection for more information.

Table 2: Survey vs. 2022 BRFSS

	Survey n=3,912	BRFSS 2022 n=125,540
Age in Years	52.30	57.98
Female	0.62	0.46
Race		
White	0.83	0.71
Black	0.07	0.09
Other	0.10	0.19
Health Insurance		
Employer-sponsored plan (own or spouse)	0.41	0.34
Individual Plan (e.g., ACA Marketplace Plan)	0.12	0.08
Medicaid	0.18	0.32
Medicare	0.17	0.09
Other Insurance.	0.04	0.11
Uninsured	0.08	0.07
Income		
Less than $25,000	0.16	0.20
$25,000-$49,999	0.24	0.25
$50,000-$99,999	0.35	0.27
$100,000-$199,999	0.21	0.05
More than $200,000	0.04	0.05
Pack-Years	27.78	21.95
Current Smoking Behavior		
Currently Smoke Cigarettes.	0.34	0.35
Recently Smoked Cigarettes (within the last 15 years).	0.37	0.25
Smoked Cigarettes, but more than 15 years ago.	0.29	0.40
Lung Cancer Screening		
Never.	0.73	0.84
Yes, but not in the past year.	0.16	0.08
Yes, in the past year.	0.11	0.08

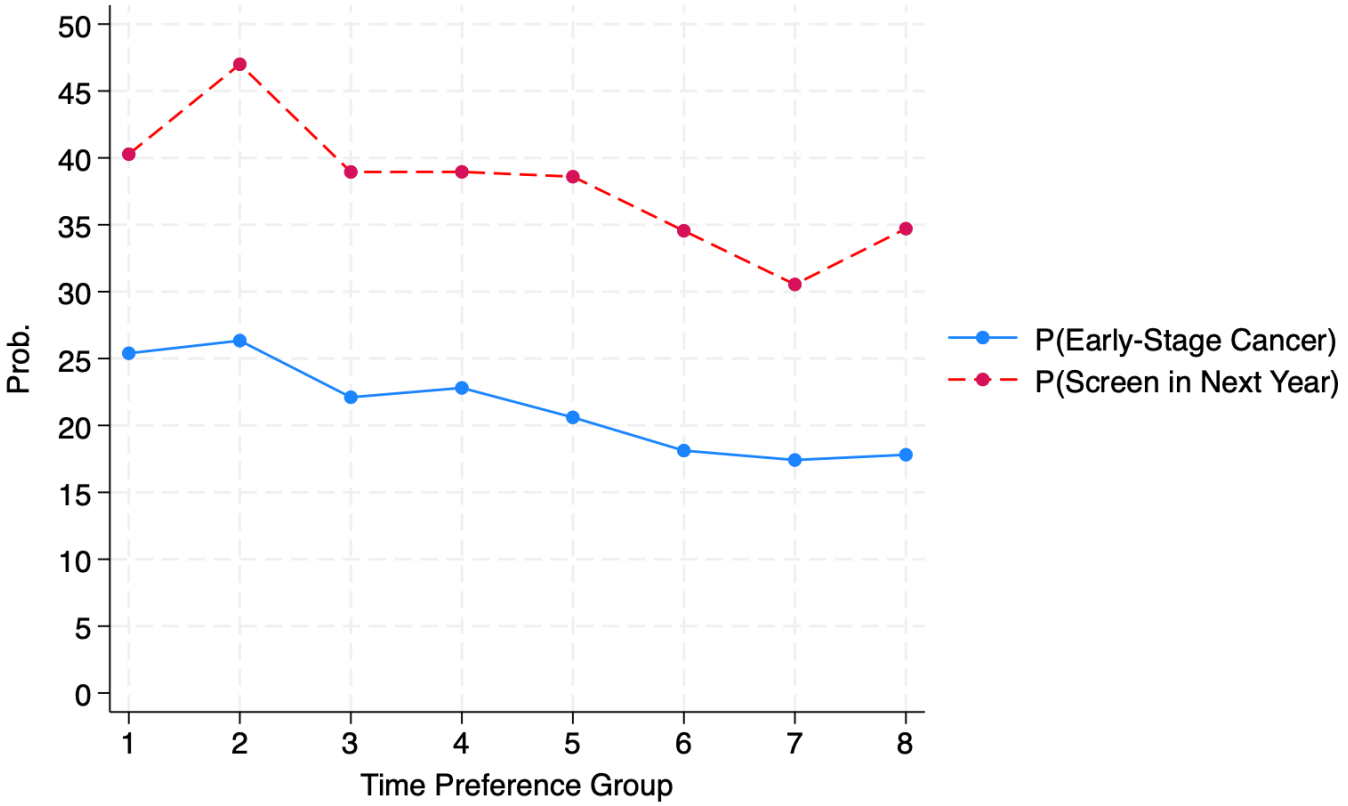
Notes: Table 2 presents overall means from our survey and from the 2022 BRFSS. As with our survey, we restrict attention to BRFSS respondents who were over the age of 40 and had some smoking history (125,540/445,132).

Figure 1: Cancer Beliefs by Risk Preference



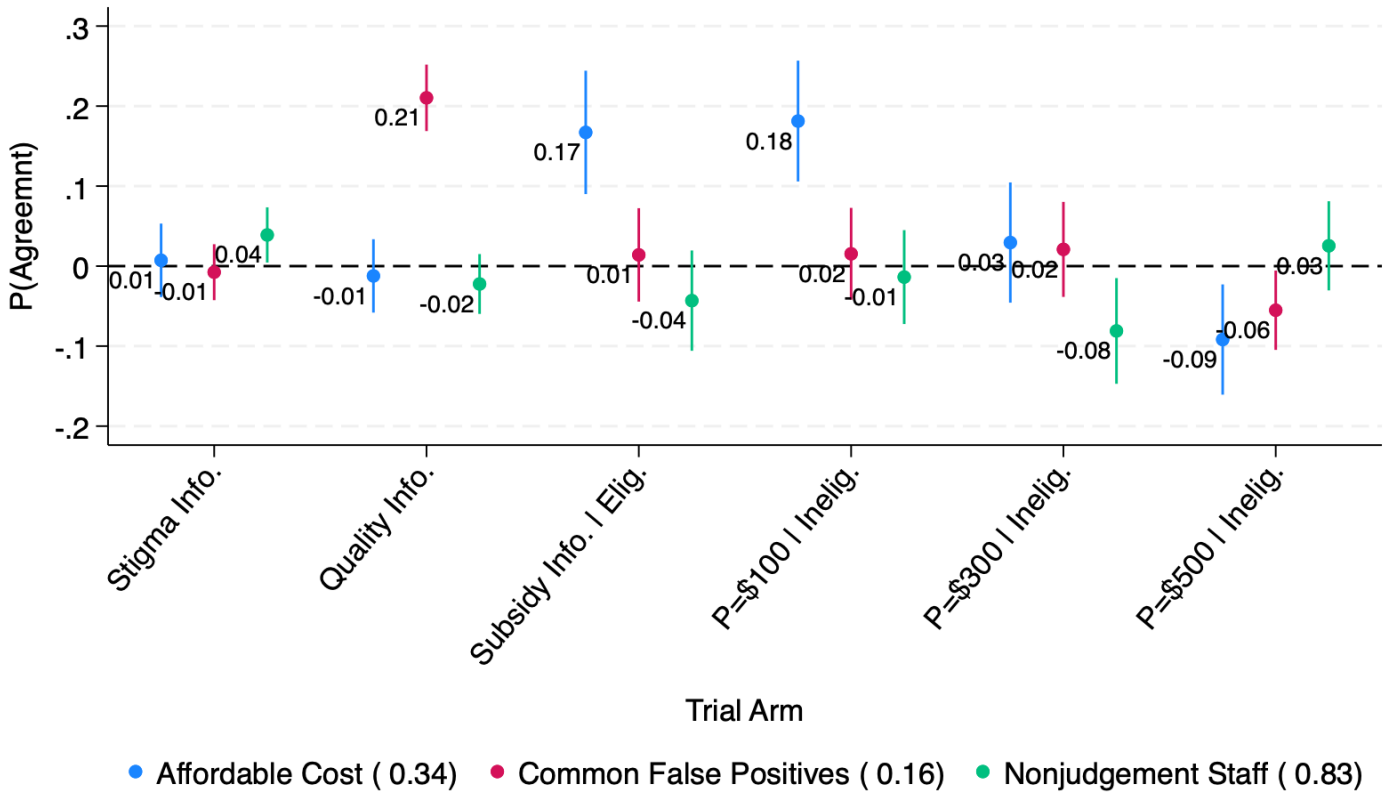
Notes: The figure presents the mean belief of early-stage lung cancer and intention to screen by risk preference group. Risk preference groups 1 through 6 reflect a CRRA risk aversion parameter in the following respective bounds: [0,0.3), [0.3,1), [1,2), [2, 3.76), [3.76, 7.53), [7.53,∞)

Figure 2: Cancer Beliefs by Risk Preference



Notes: The figure presents the mean belief of early-stage lung cancer and intention to screen by time preference group. Time preference groups 1 through 8 reflect a time consistent discount factor in the following respective bounds: [0,0.476), [0.476,0.495), [0.495,0.541), [0.541, 0.649), [0.649, 0.8), [0.8, 0.893), [0.893, 0.943), [0.943,1].

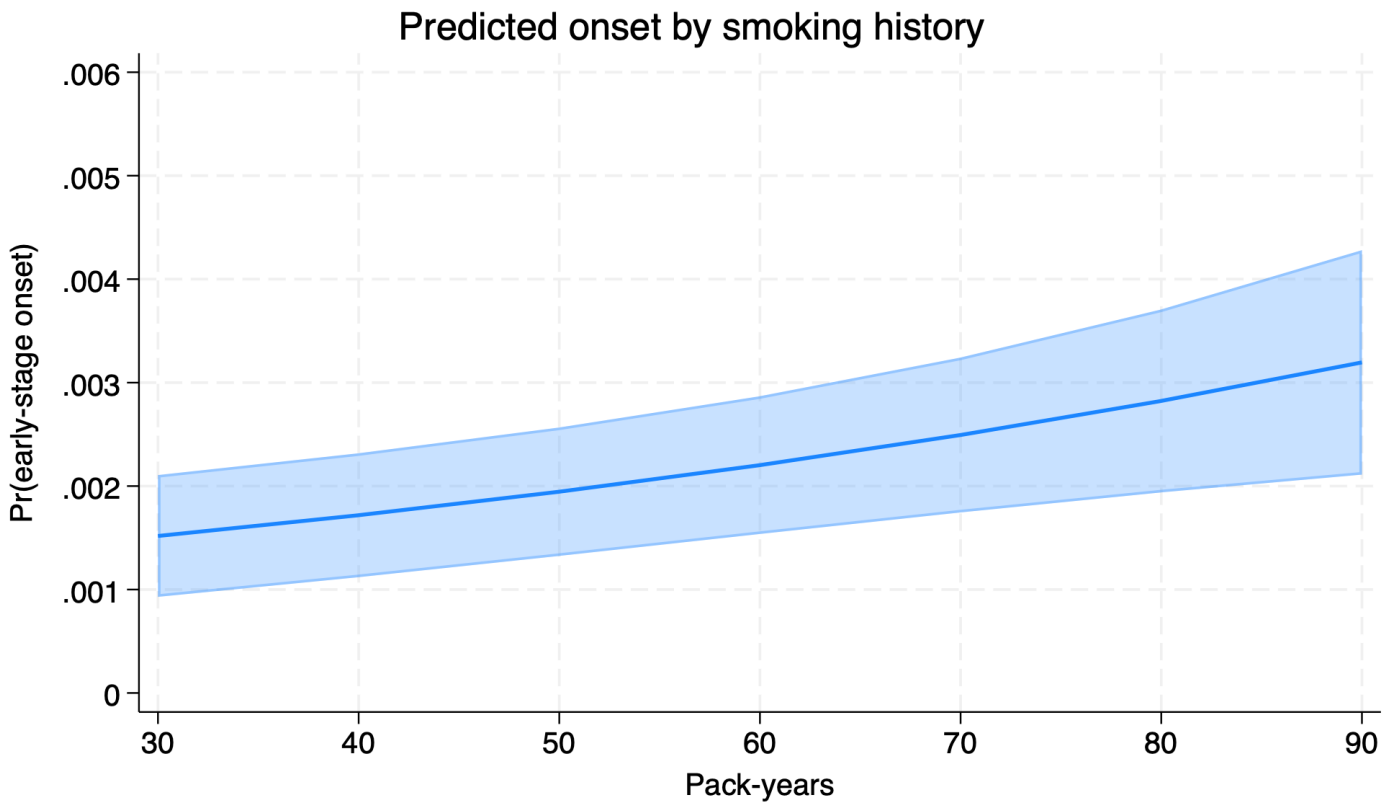
Figure 3: Comprehension Checks



Notes: The Figure presents regression coefficients of three comprehension check binary variables on binary variables for the treatment arms. The dependent variable is whether the respondent agrees that a.) screening is affordable, b.) false positive are common, and c.) screening staff are nonjudgmental. Confidence intervals reflect robust standard errors. $n = 3,268$.

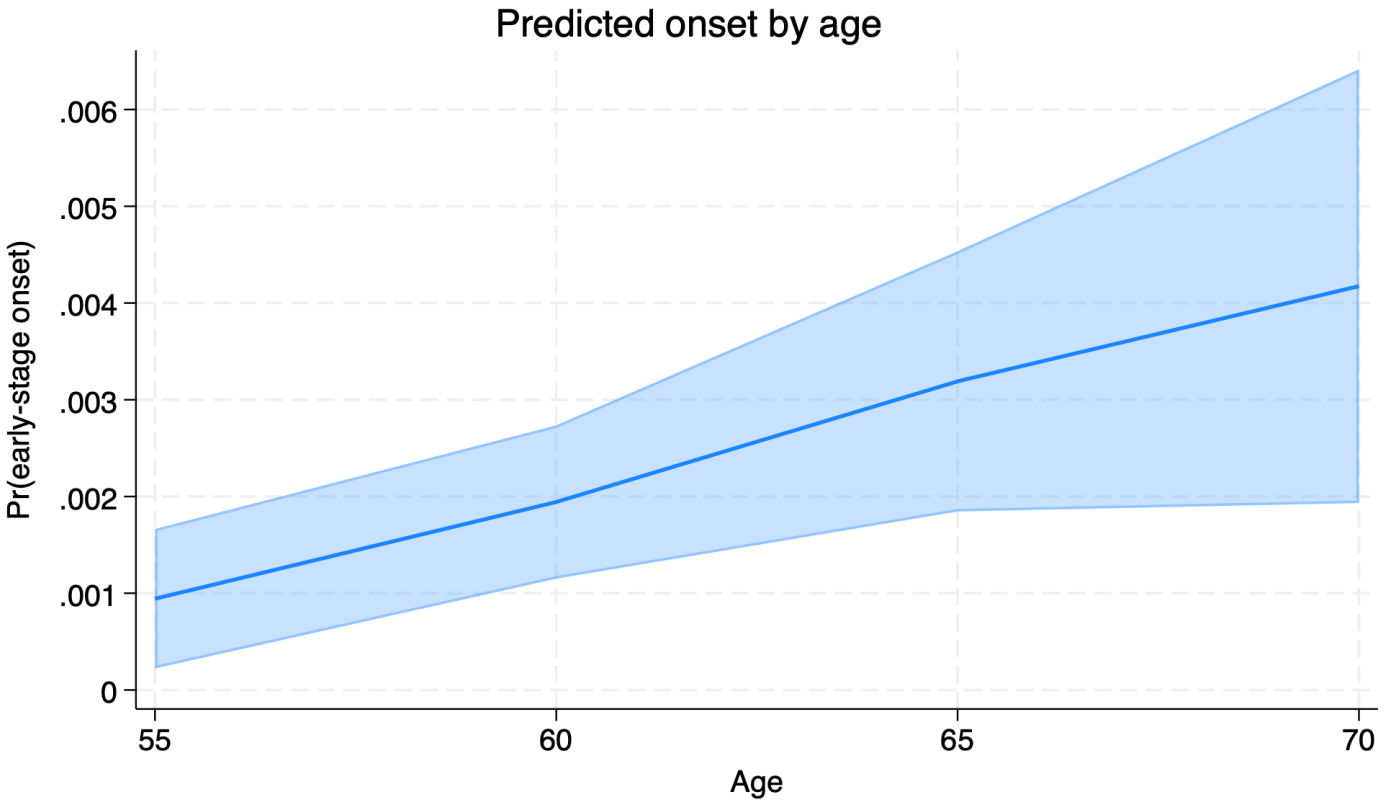
3 National Lung Screening Trial

Figure 4: Early Onset Marginal Effects by Pack-Years



Notes: Figure plots marginal effects of early lung cancer onset by pack-years. The sample is restricted those individuals who test negative, and do not realize, any lung cancer diagnoses in the first year of the trial. Onset is defined as an early-stage diagnosis in the subsequent year.

Figure 5: Early Onset Marginal Effects by Pack-Years



Notes: Figure plots marginal effects of early lung cancer onset by age. The sample is restricted those individuals who test negative, and do not realize, any lung cancer diagnoses in the first year of the trial. Onset is defined as an early-stage diagnosis in the subsequent year.

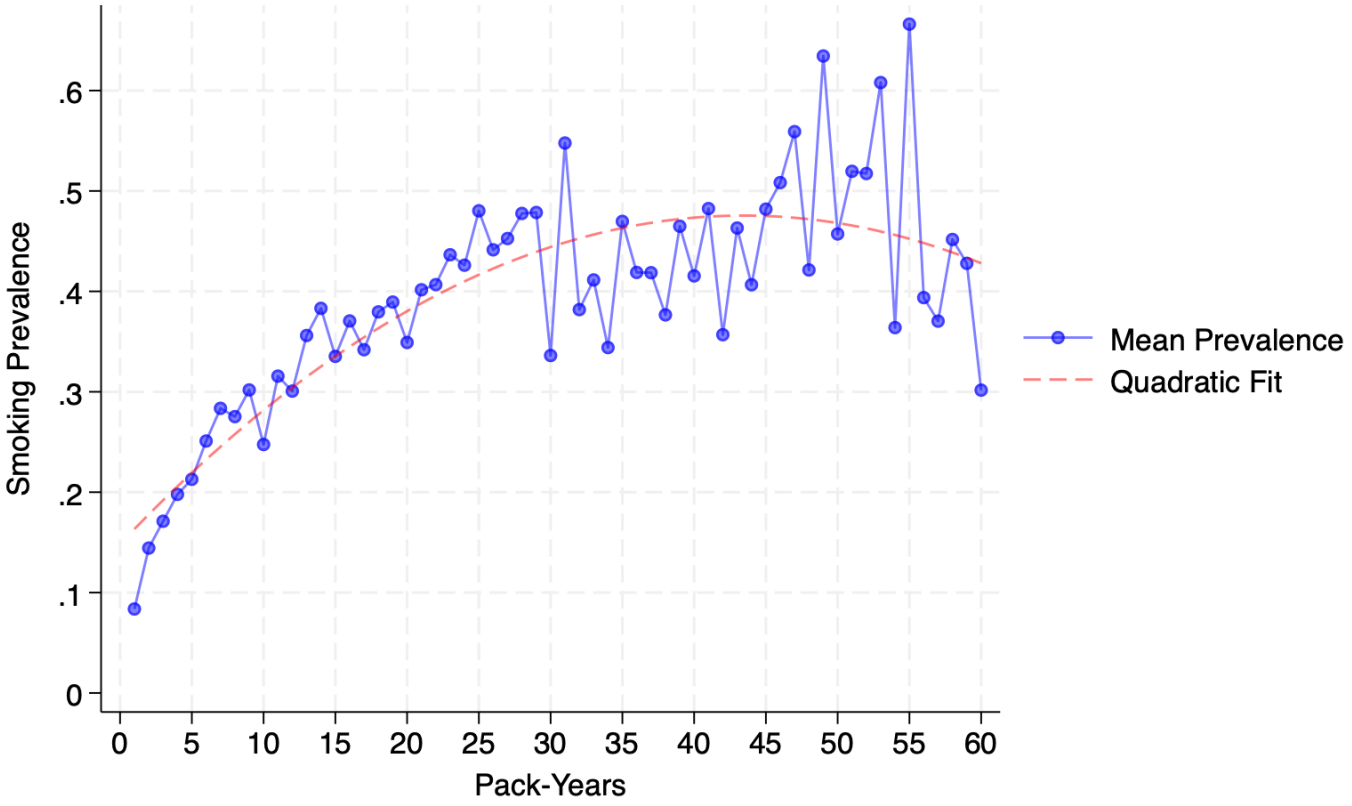
4 Behavioral Risk Factor Surveillance System

Table 3: Current Smoking and Smoking History: BRFSS

	(1) smokenow	(2) smokenow
Pack-Years/10	0.111	0.126
	(0.004)	(0.004)
(Pack-Years/10)^2	-0.009	-0.010
	(0.000)	(0.000)
Demographic controls	No	Yes
Insurance controls	No	Yes
Income controls	No	Yes

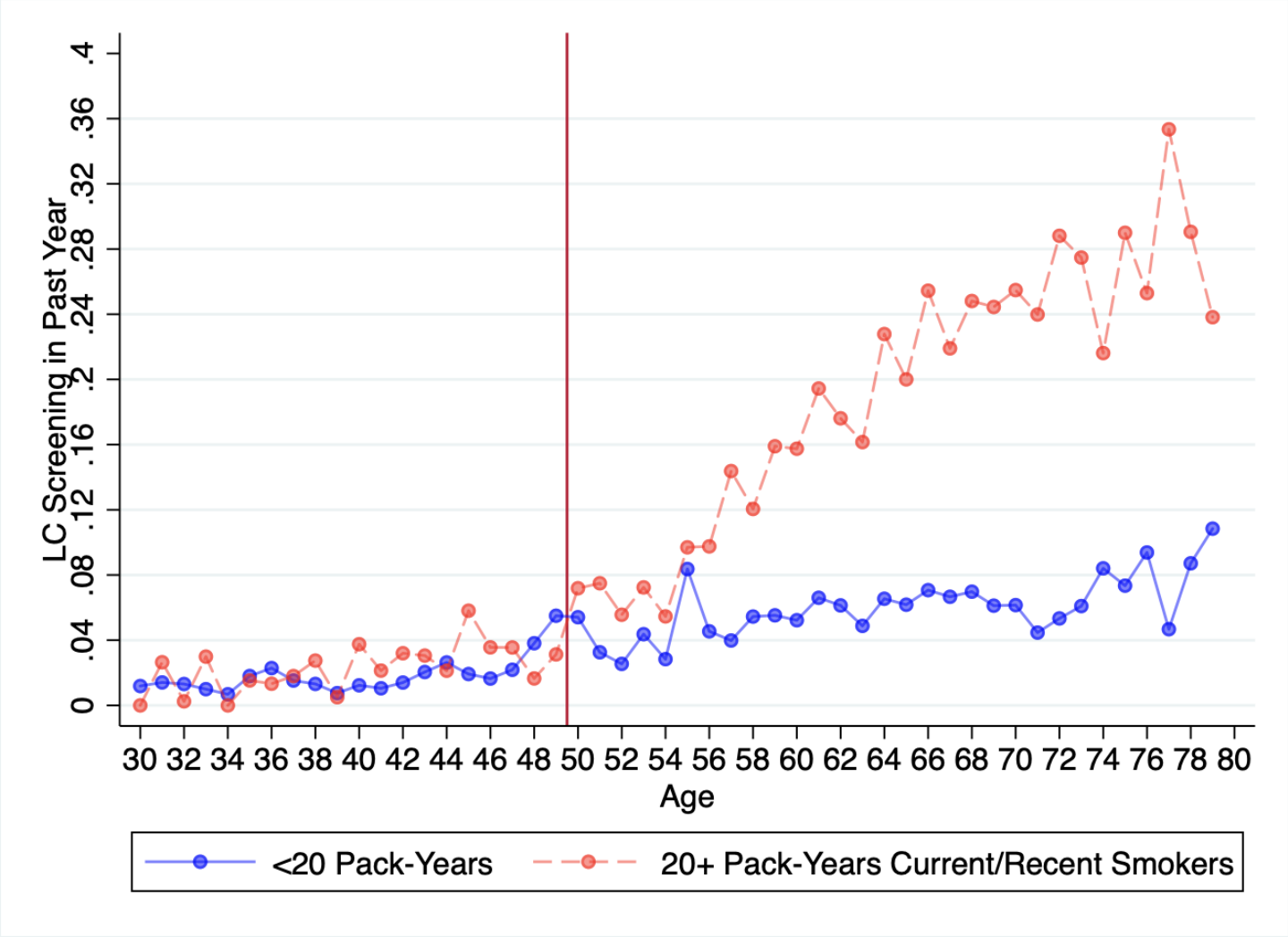
Standard errors in parentheses. n=444,685

Figure 6: BRFSS Analysis: Smoking Prevalence by Pack-Years



Notes: Figure plots smoking prevalence by the number of pack-years of smoking history as calculated by BRFSS. The best-fit quadratic line informs our utility parameters $\gamma_1 - \gamma_3$.

Figure 7: BRFSS Analysis: Screening by Age

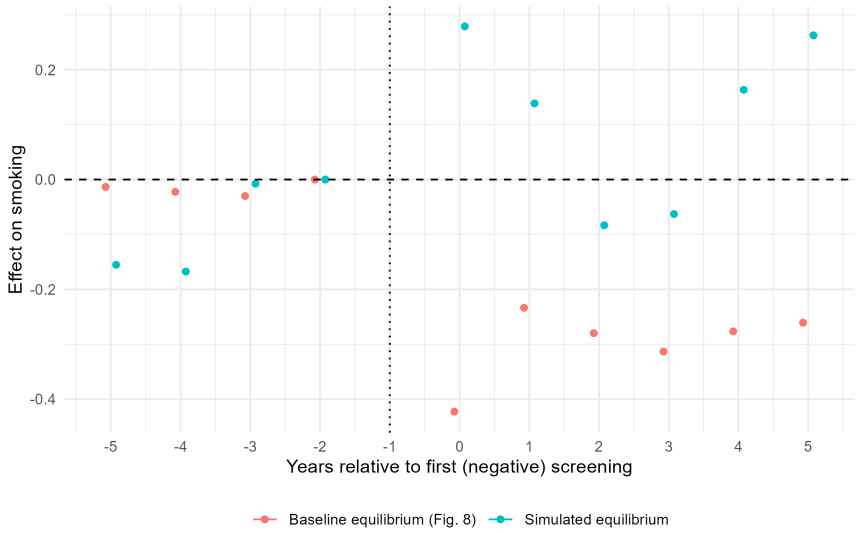


Notes: .

References

The National Lung Screening Trial Research Team (2011). Reduced lung-cancer mortality with low-dose computed tomographic screening. New England Journal of Medicine, 365(5):395–409.

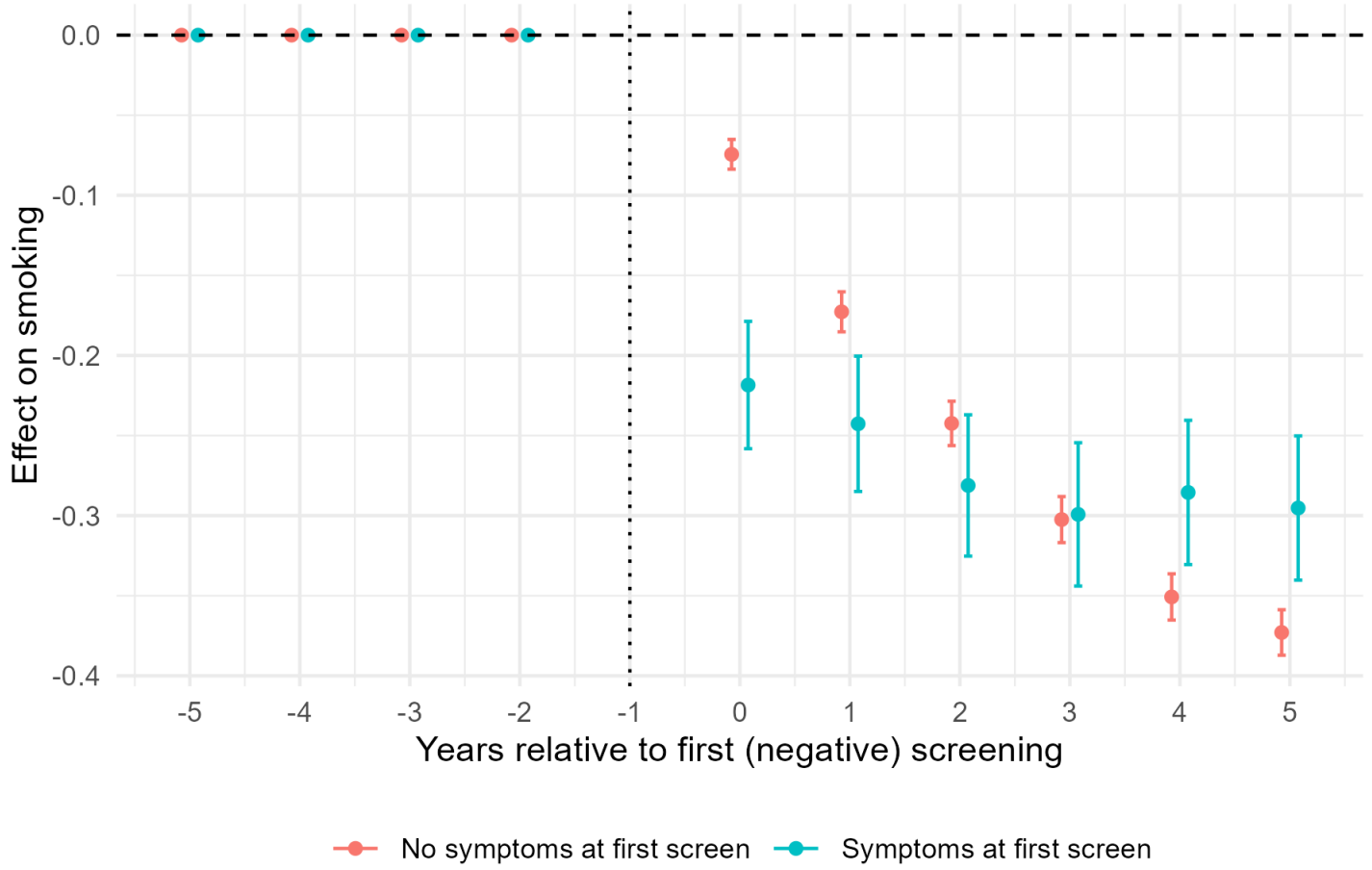
Figure 8: Simulation of the Effect of Screening on Future Smoking Decisions



Notes: Figure plots coefficients from two stacked dynamic difference-in-differences regressions estimating the effect of first screening on future smoking. The first estimation replicates the results in Figure 8, using actual equilibrium model parameters. The second estimation uses the same regression under alternative equilibrium model parameters that alter the utility from smoking, the disutility from symptoms, and the translation of symptoms into beliefs about cancer risk. Differences in coefficients across models, therefore, represent the differences in how screening affects smoking rates based on different assumptions about the data-generating process.

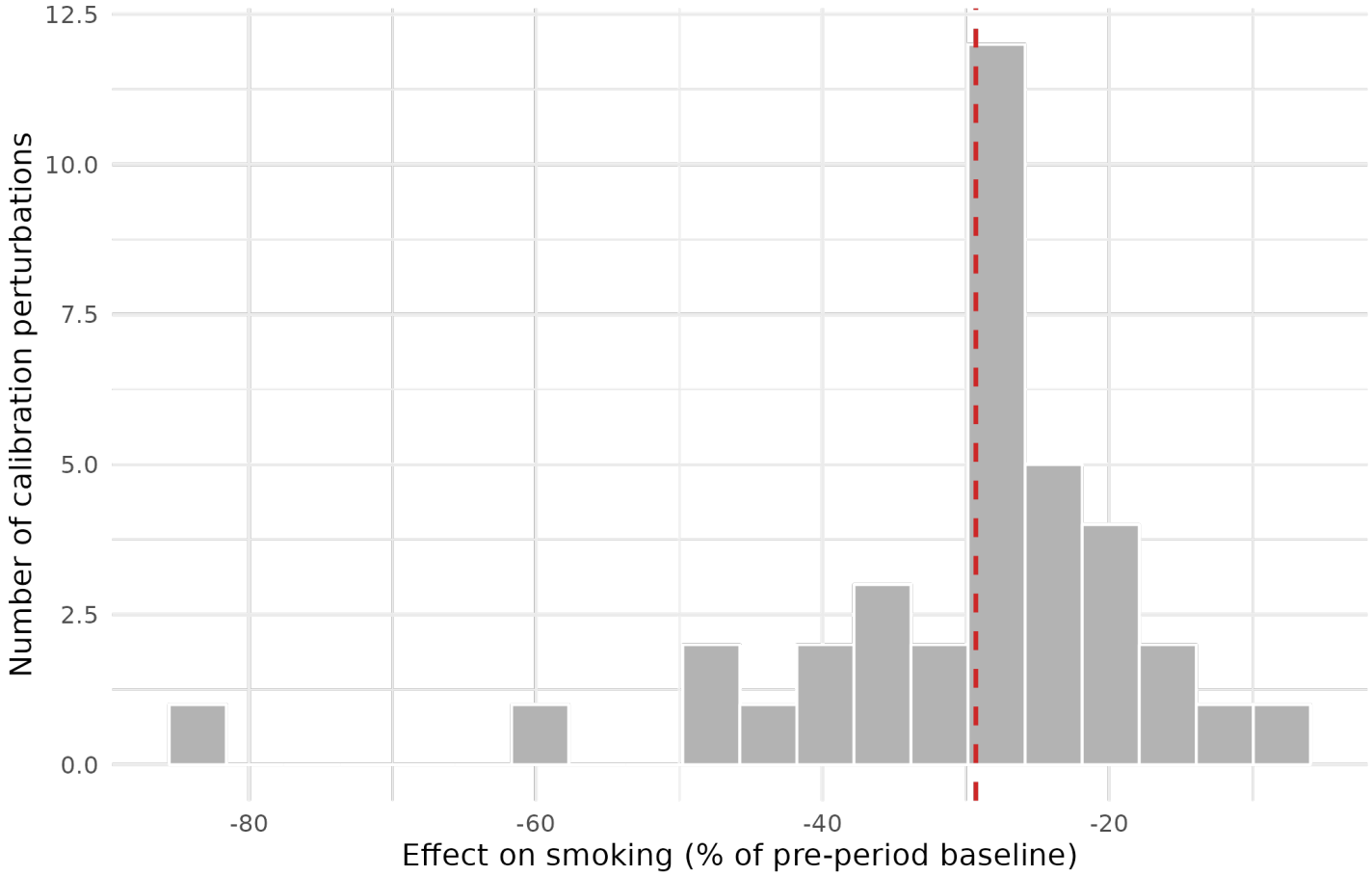
As before, each experiment is comprised of a treatment group consisting of individuals who smoked at least two years prior to their first screening, and who screened for lung cancer for the first time at age $a \in [40, 70]$; the control group consists of all individuals who also smoked for at least two years prior to age a but who did not screen for the first time until at least $a + 5$ years later. Regression adjusts for individual, experiment, and age fixed effects (note that age and experiment fixed effects are colinear) and clusters standard errors at the individual level. Point estimates therefore represent the differences in average smoking rates in the years around screening, relative to the year prior to screening and differenced relative to the clean control group.

Figure 9: Heterogeneity in Effect of Screening on Future Smoking, by Symptoms



Notes: Figure plots stacked DD coefficients following Equation (13), split by whether the screening happened in a year when the individual experienced symptoms or not. Effects are reported as the percent reduction over the pre-period baseline.

Figure 10: Sensitivity Analysis: Effect of Screening on Future Smoking



Notes: Figure plots histogram of stacked DD coefficients following Equation (13). In each simulation, we vary one of the calibrated parameters using the bounds listed in Table 3; we then resolve the model and estimate Equation (13) to identify how the effect of first screening on future smoking changes across specifications. Effects are reported as the percent reduction over the pre-period baseline. The vertical dashed line indicates the baseline result discussed in the text.